2011

Methods for increasing customization in rapid machining patient-specific bone implants

Shawn Spencer
Iowa State University

Methods for increasing customization in rapid machining patient-specific bone implants

by

Shawn M. Spencer

A thesis submitted to the graduate faculty
in partial fulfillment of the requirements for the degree of

MASTER OF SCIENCE

Major: Industrial Engineering

Program of Study Committee:
Matthew Frank, Major Professor
Frank Peters
Eliot Winer

Iowa State University

Ames, Iowa

2011

Table of Contents

List of Figures

List of Tables

Abstract

This research presents new methods for increasing the customization of the surface characteristics of rapid machined patient-specific bone implants. A bone implant is a medical device that is used for replacing missing or damaged bone tissue in a patient's body. It is possible for a bone implant to have three different types of surfaces (articular, periosteal, fracture) which each require different surface characteristics to help provide biocompatibility. It is also desirable to manufacture implants that are customized specifically for an individual patient to increase the stability and fit of the implant, which has been shown to improve patient healing. A research project at Iowa State University involves developing methods for manufacturing implants using a subtractive rapid manufacturing process called CNC-RP, which combines the automated process planning of rapid prototyping (RP) technologies with the capabilities of 4-axis CNC machining. New methods are proposed for providing more effective setup planning for the CNC-RP process, and for isolating the individual surfaces from one another during machining with the goal of increasing customization while preserving biocompatibility of the implant. The methods were used for performing setup planning for machining a bone implant using a surrogate bone material. It was shown that the methods were effective at increasing the customization of the implant, showing a notable increase in the ability to customize the fracture surface.

Chapter 1: Introduction

1.1 Background

This research involves the manufacturing of custom orthopedic implants using rapid prototyping (RP) technology. An orthopedic implant is a medical device manufactured in a way that allows it to replace missing or damaged osseous (bone) tissue inside the body (Figure 1.1.1). The goal is to allow the surrounding bone tissue to heal and integrate with the implant, a process known as *osseointegration* [1], making the implant a permanent part of the patient's body that provides strength comparable to the original, undamaged bone tissue. Orthopedic implants can be manufactured from a variety of biocompatible materials, including surgical stainless steel, titanium, metal foams, artificial bone substitutes, or natural bone harvested from the tissue of the patient or a donor.

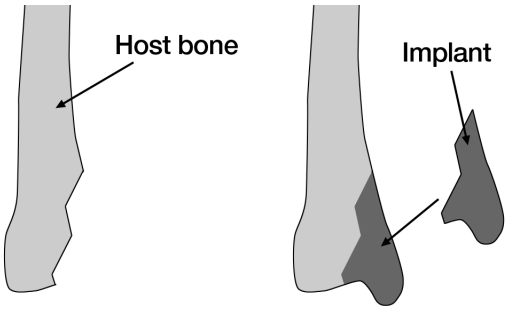

Figure 1.1.1: Bone implant

In addition to choosing proper biocompatible materials, the shape and surface finish of the implant is critical for successful osseointegration to occur. Bones requiring an implant will have mainly three types of surfaces: *articular*, *periosteal*, and *fractured*.

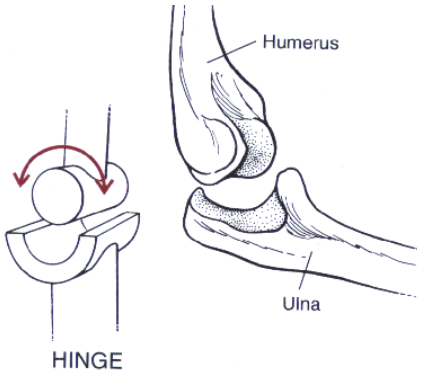

Figure 1.1.2: Joint movement [40]

An articular surface, a joint surface at which the ends of bones meet such as at the elbow or knee, is required to be as smooth as possible to reduce friction and allow safe movement (Figure 1.1.2). The bone's periosteal surface is lined with a connective tissue membrane, and should be smooth enough to allow tissue to connect, but does not need to be as smooth as the articular surface. Lastly, the fractured surface is the irregular surface of the bone that has been exposed by damage or removal of bone tissue. To aid in implant stabilization and osseointegration, previous research has shown that rough surfaces are ideal for contact with the fractured surface [8]. Rough surfaces provide friction to hold the implant in place, while providing small pores for new bone tissue to grow into and interface. Depending on the location and type of injury, it is possible that a single implant would be required to have surfaces of all three types (fractured, periosteal, articular). A custom manufactured implant would need to have a rough surface corresponding to the fracture location of the host bone, along with surfaces that allow for continuation of the articular and periosteal regions.

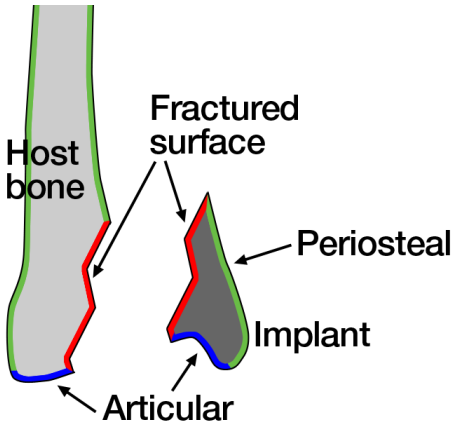

Figure 1.1.3: Different types of implant surfaces

The unique nature of bone injuries between different patients means that orthopedic implants can be widely varied in shape and surface finish requirements. This often requires an orthopedic surgeon to handcraft a custom implant to suit a particular patient's injury site. During the operation, the surgeon will often make small

adjustments to the shape of the implant, compare it with the planned implant site, and then iterate this process until a nominal fit is achieved. In order to reduce some of the uncertainty and inaccuracies in this process, and to help reduce the invasiveness of the surgical procedure, it would be beneficial to manufacture the implants according to medical imaging data obtained from the patient [21]. Previous research has also demonstrated that implants that provide a more stable and accurate fit allow for better healing and patient recovery [5]. Highly accurate 3-dimensional (3D) models of the patient's implant can be constructed from medical imaging data, such as that achieved through computed-tomography (CT) data. To create a more effective implant, a machine is needed that would be able to quickly and easily manufacture the implant according to the 3D model.

The challenge in manufacturing these implants is in development of a process that allows for the creation of highly customized parts with varying surface roughness in select locations. Using current conventional manufacturing methods, such as casting, molding, conventional machining, etc., requires the labor of a group of highly skilled technicians that have specialized knowledge of how to manufacture the parts. Before the actual part can be made, a significant amount of time and labor must be spent in pre-process engineering and planning, such as choosing effective setups, creating custom fixtures, planning the sequence of operations, and selecting the appropriate tools. In an environment where each part being manufactured is customized and significantly different than the one before it, these pre-process planning steps would need to be repeated for each and every part. This poses a problem as demand for

custom orthopedic implants increases, in that the vast majority of the time and cost associated with making the implant is spent on planning and setup; which requires the attention of those skilled technicians, a resource which is usually limited in a production environment. One of the goals of this research is to enable custom bone implants to be manufactured using an automated, push-button process that eliminates the need for the pre-process engineering and skill required to produce the part by conventional methods. Such a process would allow a manufacturer to go directly from computer-aided design (CAD) model to making the implant, without the manual setup planning in between. As demand for implants increases, the only resource needed would be machine time, and an effective automated process could allow machines to run around the clock, meeting demand for parts in a timelier manner than current conventional methods. Moreover, it is hoped that a computer controlled manufacturing process, utilizing accurate CT derived models, would be able to improve the accuracy of fit and function for the resulting implant, as compared to handcrafting in surgery.

1.2 Rapid Prototyping Overview

Rapid prototyping systems utilize a highly automated layer-based manufacturing process that allows the user to create a part directly from a CAD model. RP technologies first emerged in the 1980's, and have grown in use for their ability to create complex parts from CAD data. The setup planning process is automated by computer software and involves slicing the model into cross sectional layers. For example, using RP technology a custom Lego brick could be easily made from a CAD

model, without taking the time to create an injection mold for the part. The surface of the CAD model is first converted into a collection of triangular facets—a process known as tessellation.

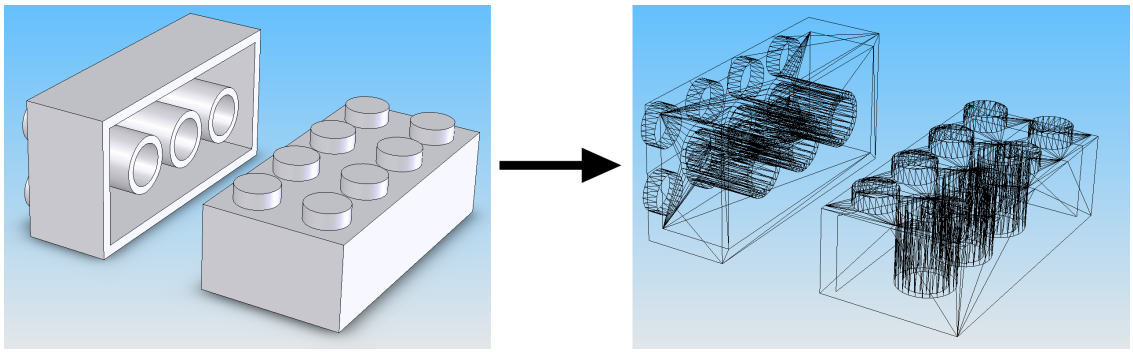

(a) (b)

Figure 1.2.1: a) 3D CAD model of a Lego brick. b) The Lego brick model after tessellation, with surface represented by triangular facets.

Once the model is tessellated, it is sliced into 2-dimensional (2D) cross sections by intersecting planes at varying positions along the z-axis. The triangular facet representation is convenient because it simplifies the math required for finding the surface/plane intersection, and allows for the use of a simple yet robust slicing algorithm on complex models. The outline of each slice is drawn by tracing the line of intersection between the slice plane and the triangular facets of the model.

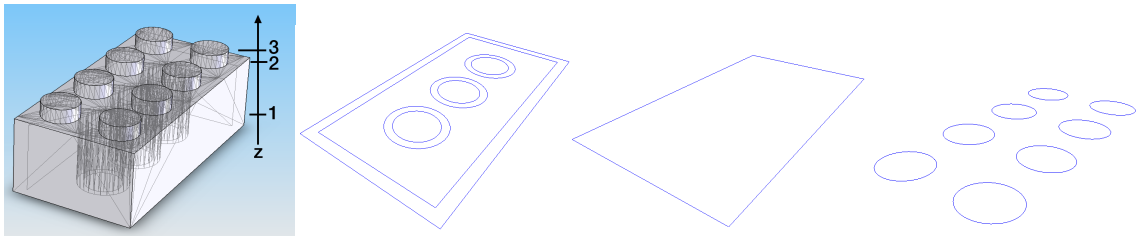

(a) (b) (c) (d)

Figure 1.2.2: a) Lego model to be sliced at three different positions along the z-axis. b) Slice 1 from Lego model. c) Slice 2 d) Slice 3

A machine utilizing a numerically-controlled material deposition nozzle, traveling in the x-y plane, can then fill material within the boundaries of the 2D slices. This process is repeated, with the machine depositing a new layer of material on top of the previous layer, until all layers have been built and the part is finished.

There are many different RP processes available commercially, with most of them falling under the category of *additive* manufacturing methods. Additive RP processes—such as stereolithography, 3D printing, fused deposition modeling (FDM), and selective laser sintering—involve building up layers of material by depositing new material on top of the layer below, where each layer has a shape corresponding to a cross-section of the CAD model. Additive processes are possible with specialized materials that have been found suitable for depositing small layers, with each layer joining properly with the layer below.

Conversely, *subtractive* processes begin with a piece of stock material that is larger in overall size than the part that will be manufactured. Material is selectively removed from the stock piece with a cutting tool, leaving the desired geometry when complete. Subtractive processes mainly utilize numerically-controlled milling or turning procedures for removing material. Subtractive manufacturing has seen very limited use in rapid prototyping, mostly relegated to small desktop milling machines. A current research effort at Iowa State University is developing a more advanced subtractive RP technology called CNC-RP [25].

1.3 Overview of CNC-RP

Computer numerical control rapid prototyping (CNC-RP) is a subtractive process that combines the automated process planning of RP technology with the capabilities of 4-axis CNC milling to create parts from CAD models. In contrast with additive RP technologies, CNC-RP allows for the use of many new materials that can be acquired in stock form, including FDA-approved biomaterials like natural coral, titanium foam, and biocompatible polymers. CNC-RP utilizes a layer-based computer algorithm that analyzes the geometry of the CAD model and finds which part surfaces are visible from different orientations. Beginning with material in round stock form in a 4th axis rotary indexer, the CNC mill machines all surfaces that are visible from a particular setup orientation, after which the indexer rotates the work piece to a new position, allowing the cutting tool to access surfaces that were inaccessible during the previous orientation (Figure 1.3.1). This process is repeated until all surfaces of the CAD model have been machined, with the desired part geometry remaining. The automated setup planning algorithm chooses the orientations that allow for complete coverage of the part, while reducing the total number of required rotations.

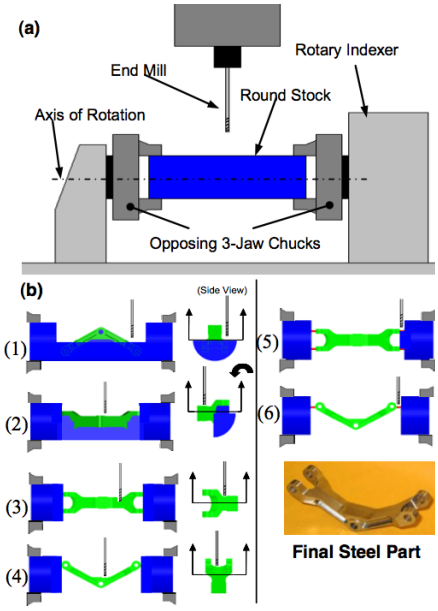

Figure 1.3.1: Steel part machined from four different orientations.

Previous research has shown that CNC-RP is effective for producing functional industrial components—parts that have been traditionally cast or machined from steel or aluminum. The resulting parts have good dimensional accuracy and strength, allowing for the creation of functional replacements for parts that have broken down. While the results have been positive when producing industrial parts with CNC-RP, new challenges arise when using it to manufacture orthopedic implants.

The process planning algorithm of CNC-RP examines triangular mesh models of the parts being manufactured, commonly in the STL file format. The triangular facets of the model represent the shape and dimensions of the part. The objective is to ensure that all points of the model that are visible from a particular orientation have been machined. To assess the visibility of a point from a specific orientation, the CAD model is sliced into two-dimensional cross sections, after which the points of each cross section are tested for visibility. During the slicing and visibility test, all points and facets of the model are assumed to represent the same material and surface properties, with the desired result being a manufactured part that has the same shape and dimensions as the model.

In manufacturing orthopedic implants, there is not only the need for replicating the shape and dimensions of the model, but also selective customization of the surface finish of the material. In this case, all points on the CAD model cannot be assumed to have the same properties, requiring a method of customizing the surface properties within select regions of the part. The CNC-RP process needs to target specific surface regions within each orientation, while taking steps to avoid surrounding regions of

different surface properties that should not be interfered with. For example, when machining the fractured surface of a bone implant, it is important to make sure the cutting tool stays within the appropriate region, and does not inadvertently touch nearby joint surfaces.

1.4 Selective Customization of the Part Surface

The need has been established for CAD models that represent multiple materials or surface data in a single part. In biomedical applications, such models could be utilized in an integrated system for printing different types of biomaterials that would bond and interact with one another to form a complex artificial organ. In manufacturing orthopedic implants, the definition of multiple types of CAD surfaces would correspond to the periosteal, articular, and fractured regions of the implant. In these types of applications, each surface of the model would need to have a clear definition of the boundaries between neighboring material regions.

This research expands on methods developed by Joshi [19] for targeting custom surfaces in CNC-RP. In Joshi's work, polygonal CAD files in the PLY file format were used for process planning. The PLY files contain the definition of triangular facets that have associated color information for representing different types of surfaces. Facets that are red represent the fractured surface, green is periosteal, and blue is the articular surface. The model is sliced into cross sections (Figure 1.4.1), with

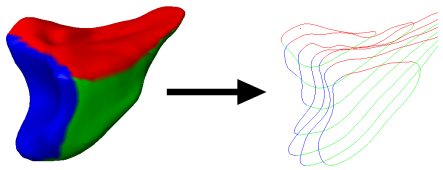

Figure 1.4.1: Colored model, and cross sectional slices.

each segment of the slice assigned a color corresponding to the type of implant surface at that particular location. The points on each slice are tested for visibility from different orientation angles. An objective function is used with the goal of choosing setup angles that isolate the different types of surfaces (different colored points of the slices), while also providing full coverage of the part geometry. In Figure 1.4.2a, the machining angles generated from the previous method are shown, in which all surfaces of the part are assumed to be the same. Figure 1.4.2b shows the setup angles found using Joshi's method, which creates setup angles that better isolate the different surfaces of the part.

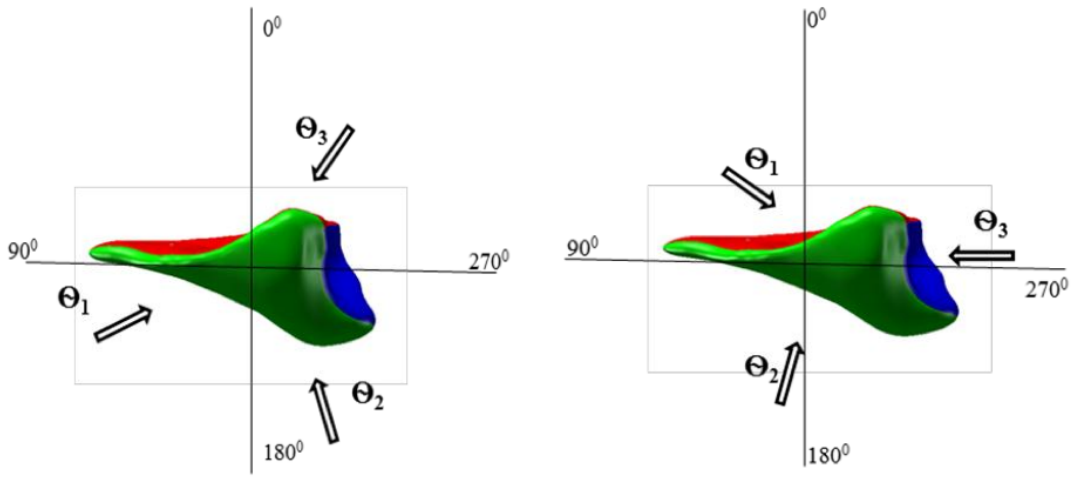

Figure 1.4.2: a) Machining setup angles preventing surface customization. b) Setup angles that allow for surface customization by isolating different implant surfaces.

Limitations were noted in cases where the surfaces could not be completely isolated from one another. A setup orientation that was meant for machining only the articular surface would overlap with geometry of a fracture surface, causing the fracture surface to be machined partially. This problem is referred to as *tool path cross*

over (Figure 1.4.3). This is a problem because inadvertent machining of different nearby surfaces can reduce the effectiveness of the orthopedic implant. For example, if a surface that is meant to have a rough finish is inadvertently machined smooth by tool paths that cross over into this area, it could reduce the friction at the bone-implant interface, which has a negative effect on implant stability and patient healing.

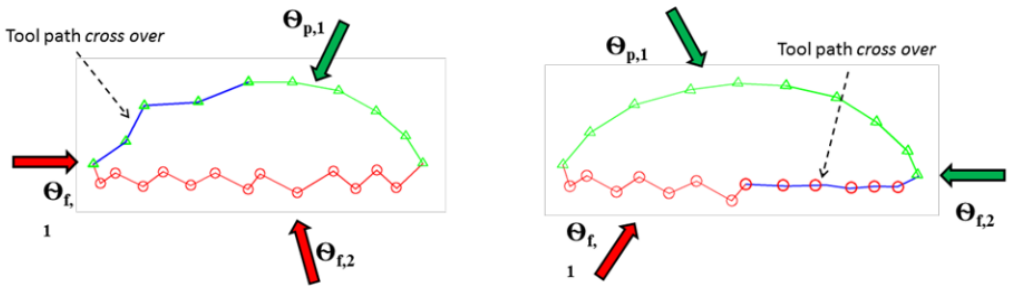

(a) (b)

Figure 1.4.3: Tool path cross over. a) Tool paths meant for only the green (periosteal) surface will overlap onto the blue (articular) surface. b) Tool paths will overlap from red (fractured) surface onto blue (articular) surface.

This thesis proposes new methods for obtaining greater control and accuracy in creating customized surfaces using CNC-RP. It addresses two basic objectives: 1) How can one more accurately provide slice data for initial setup planning and 2) Given a set of setup angles, how can one ensure that the individual surfaces are machined independently? In doing so, this work considers the overarching problem of ensuring that the biocompatibility of the implant is maintained and optimized. For the first problem, providing accurate slice information, this thesis presents a method of modifying the initial slice data if ambiguous surface boundaries are found (uncertainty in the form of "noise", with respect to boundary type). To address the second problem, ensuring surfaces are independently machined, this work presents a method for

creating tool path containment boundaries that restrict the tool from machining neighboring surfaces. In both methods, we actively address the issue of biocompatibility by sequentially giving priorities to the 3 major surfaces where modifications to the slices, or boundaries for tool paths are chosen based on the type of surface it is modifying. This method will allow the user to safely and selectively customize the material properties on the surface of the part, compensating for inaccuracies in using 3D scan data to perform process planning for a CNC milling process.

1.5 Thesis Organization

The layout of the remainder of this thesis is described as follows. *Chapter 2* provides a literature review of research that studied the effects of bone implant surface roughness on bone healing and the osseointegration process. Other research is shown on techniques for processing colored CAD models, RP processes for multi-material parts, triangular mesh segmentation techniques, and their respective advantages and limitations. *Chapter 3* details the new methods for processing colored bone implant models for improved customization of surface roughness in the CNC-RP process, and is presented in paper format. *Chapter 4* presents the general conclusions from this research and discusses opportunities for future work.

Chapter 2: Literature Review

2.1 Biomedical Implant Manufacturing and Aiding Bone Healing

Extensive research has been performed in developing the materials and manufacturing methods used for creating effective bone implants. Materials used in bone implants need to be biocompatible, and thus implants are commonly made from materials such as titanium, tantalum, stainless steel, polymethylmethacrylate (PMMA, also referred to as bone cement), and various other biocompatible polymers and ceramics. Considering the unique, free-form shape of biomedical implants, and the desire to create custom implants, many layer-based additive manufacturing methods have been utilized [2, 3, 13, 31]. These methods include fused deposition modeling (FDM), 3D printing, stereolithography, electron beam melting, and laser engineered net shaping (LENS). Melchels et al. [2] evaluated the effectiveness of stereolithography in biomedical applications, and demonstrated that bone implants could be created that were useful in surgery planning. They also noted that stereolithography had uses in many other biomedical applications such as tissue engineering scaffolding and custom hearing aids. Espalin et al. [3] demonstrated the effectiveness of using FDM to create craniofacial implants out of medical-grade PMMA while approximating the original tissue densities and porosity. A femur model was also fabricated. While the form and fit of the fabricated models were effective, it was noted that the strength of the models could be negatively impacted depending on build direction and porosity.

In bone implant surgeries, a primary concern is the fixation stability of the implant, and the ability for the surrounding bone tissue to react positively with the implant material [17]. An effective bone implant will allow for osseointegration, meaning that living bone tissue grows directly on and around the implant [1, 18], integrating the implant as a permanent part of the patient's body. Research has been demonstrated on the effect of surface properties in orthopedic implants and dental implants on osseointegration, in both humans and animals [6-11]. It was shown that implants made with rough, porous surfaces located at the bone-implant interface are highly effective at aiding osseointegration and bone ingrowth. Titanium dental implants that had been roughened using grit-blasting, acid-etching, or anodizing had significantly higher rates of bone ingrowth and stability than those left untreated [6, 9, 10]. Trabecular metal (a type of metal foam) has been utilized in bone implant research because it provides pores for bone tissue to grow into. Deglurkar et al. [7] demonstrated that when trabecular metal implants were machined, the pores were smeared and closed, resulting in less bone ingrowth and a less effective implant. Research has been performed regarding methods for machining trabecular metal without smearing and closing the pores [4]. Using an infiltrant, the smearing was greatly reduced during machining, and the pores were preserved. It was proposed that the infiltrant could also act as a barrier that prevents contaminants from entering the implant during manufacturing.

In total hip replacement surgery, the majority of implants are fixated without the use of bone cement [20]. Early research by Albrektsson et al. [14] showed evidence

that osseointegration could occur in humans without the use of cement, using threaded titanium screws. Tight initial fixation stability was noted as a primary requirement for ensuring permanent osseointegration, and preventing tissue irritations at the implant interface [5, 14, 15]. It has been estimated that around 5-10% of hip replacements fail within the first 10 years, and it has been shown that micromotions at the bone-implant interface are a primary cause [13]. Micromotions are microscopic movements between the implant and bone surface. These motions are often difficult to detect, and can lead to loosening of the implant over the long term. In order to maintain high initial fixation, and a reduction in motion at the bone-implant interface, a high amount of friction is desirable at the interface [12, 16]. Hsu et al. [16] demonstrated that micromotion increased as friction between the implant and bone surfaces decreased. It was shown that an implant surface with a coefficient of friction of 0.5 or above could reduce the motions by over 20%, which lead to an increase in bone ingrowth.

2.2 Processing 3D CAD Data for Biomedical Objects

As noted by Thomas et al. [21], surgeons are faced with a difficult challenge when reconstructing complex bone fractures. Often, they iteratively modify the bone fragments during the surgery, until it is judged that a good fit has been achieved. In order to remove some of the uncertainty and inaccuracies from this process, it is desirable to manufacture the implant according to medical imaging data. To assist in this process for highly-fragmented bone fractures, Thomas et al. has demonstrated a 3D puzzle-solving application for creating accurate CAD models of bone implants.

In order to utilize computer-aided layer-based manufacturing methods, a 3D CAD model of the implant is needed, and the model will need to be sliced into cross sectional layers for process planning. Several different approaches can be taken for representing the geometry and material properties in the CAD model and slices. Triangular mesh models in the STL file format are commonly used in RP applications to represent the geometry of 3-dimensional objects. In order to represent models with differing colors, materials, or material properties, modified STL files have been used that include color information in addition to geometry definition [32-36]. This is useful in biomedical applications for differentiating between different types of biomaterials, and other applications such as modeling parts made from functionally graded materials. Choi and Cheung [32-34] have developed a virtual prototyping system for visual simulation of the manufacturing of multi-material objects, and also biomedical objects such as bones, simulating an additive method similar to FDM. Assemblies of STL models were used for representing the different components of the parts, with each component of the assembly having a different color if representing a different type of material (or different material composition). The models were sliced, with different colored slice contours defining where the different materials were to be placed in the layer. Although no physical parts were manufactured, the virtual prototyping method was noted as being useful for identifying process planning challenges, and also for identifying areas of unacceptable dimensional deviation stemming from slice thickness or build direction.

Aside from using slice contours for defining material deposition locations, a common approach in 3D printing is to represent the layer information using voxels. Wang et al. [36] outline a method for slicing colored STL files, and constructing colored voxel information from the colored slices. The colored voxels in each layer could then be used to direct an inkjet head to deposit colored ink in select locations during 3D printing, similar to printing the pixels of a 2D image. The voxel information was a direct approximation of the triangular facets of the model, without attempting to compensate for cases of low-resolution meshes.

Zhou et al. [37] describe a method for modeling and processing parts designed with functionally graded materials. The geometry of the part was described using conventional CAD representations, but the differing material composition was represented by a distance function dependent on the distance from the surface of the part in a particular direction. When slicing for RP, the material composition functions are associated with the geometry of each slice. The continuous material function can then be converted into discrete voxels of material data concurrently when depositing the material of the slice.

It has been noted that constructing 3D CAD models from medical imaging data that are suitable for RP is often still a complicated and laborious task, and research is going into creating a simpler and more robust procedure [35]. Wang et al. propose new methods for creating STL models directly from CT image data, while ensuring that the model does not contain holes and gaps. Data points from each layer of the CT data was examined using a statistical prediction method for accurately identifying closed

boundaries in the scanned objects, and generating triangular facets that map to these boundaries.

STL models are generally an unstructured, unorganized collection of triangular facets, and work has been done by Kim et al. [38] to identify a hierarchy of components in the model, and to sort the facets into an assembly structure. Examples were given with model of a cell phone, in which the proposed method could identify the different components of the phone (keypad, screen, etc.) and segment the mesh accordingly. The segmentation was based on analyzing surface normals, and iteratively joining topographically related facets into larger components. An adaptation of methods developed by Latecki and Lakämper [39], which are used for identifying shapes in 2D images independent of image noise, were utilized for smoothing out the boundaries of the segmented components based on decomposing the boundary shapes into convex components.

2.3 Machining in Biomedical Applications, and Rapid Machining

Hieu et al. [28-30] have developed methods for designing and manufacturing implants for custom cranioplasty applications. It was desired to manufacture custom-molded PMMA implants. 3-axis CNC milling was used for making custom molds, not for machining the implants directly. Molds were created using 3-axis CNC milling, and later filled with PMMA to create the implant. The study was largely successful at creating custom implants for cranioplasty, although limitations were noted in the complexity of the implants that could be achieved by a molding process.

A rapid process has been developed by Frank et al. [23-25] for using 4-axis CNC milling for directly machining parts out of round stock material for both industrial and biomedical applications. This new method, referred to as CNC-RP, creates the opportunity for using many new and different materials that are available in stock form that may not have been suitable for use in additive RP processes. To determine the setup orientations for positioning the part in the 4^{th}-axis rotary indexer, the CAD model is sliced and the points of each slice are analyzed for visibility from different orientations. A greedy set cover algorithm is utilized for determining an efficient number of the setup orientations that maximizes visibility of all points of the part surface. During this process, all surfaces of the part are treated as having the same surface properties, and same surface finish. When using the CNC-RP process for manufacturing bone implants, the need was presented for representing different surface regions (articular, periosteal, and fracture surfaces) within the implant model, and for aiming setup orientations at the individual surfaces. A revised process planning method was developed by Joshi [19] for utilizing colored slice data (originating from colored models in the PLY format), for determining setup orientations that would better isolate the surfaces. The different colors in each facet and slice segment correspond to the type of surface represented. This version of CNC-RP, which is tailored towards biomedical applications, is referred to by the authors as CNC-RP_{bio}.

Chapter 3: Methods for Increasing Customization in the Rapid Machining of Patient-Specific Bone Implants

3.1 Introduction

This research involves the manufacturing of custom orthopedic implants using rapid prototyping (RP) technology. An orthopedic implant is a medical device manufactured in a way that allows it to replace missing or damaged osseous (bone) tissue inside the body (Figure 3.1.1). The goal is to allow the surrounding bone tissue to heal and integrate with the implant, a process known as *osseointegration* [1], making the implant a permanent part of the patient's body that provides strength comparable to the original, undamaged bone tissue. Orthopedic implants can be manufactured from a variety of biocompatible materials, including surgical stainless steel, titanium, metal foams, artificial bone substitutes, or natural bone harvested from the tissue of the patient or a donor.

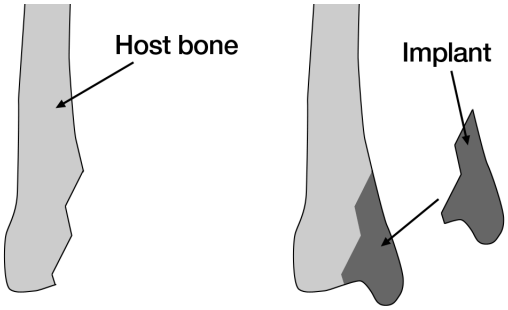

Figure 3.1.1: Bone implant

In addition to choosing proper biocompatible materials, the shape and surface finish of the implant is critical for successful

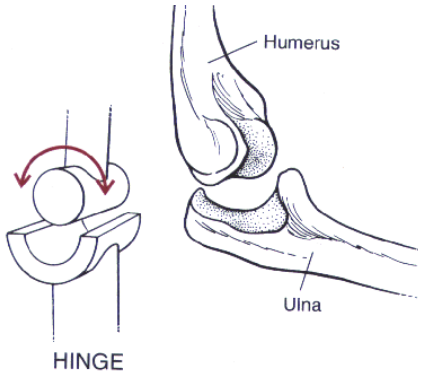

Figure 3.1.2: Joint movement [31]

osseointegration to occur. Bones requiring an implant will have mainly three types of surfaces: *articular*, *periosteal*, and *fractured*. An articular surface, a joint surface at which the ends of bones meet such as at the elbow or knee, is required to be as smooth as possible to reduce friction and allow safe movement (Figure 3.1.2). The bone's periosteal surface is lined with a connective tissue membrane, and should be smooth enough to allow tissue to connect, but does not need to be as smooth as the articular surface. Lastly, the fractured surface is the irregular surface of the bone that has been exposed by damage or removal of bone tissue. To aid in implant stabilization and osseointegration, previous research has shown that rough surfaces are ideal for contact with the fractured surface [8]. Rough surfaces provide friction to hold the implant in place, while providing small pores for new bone tissue to grow into and interface. Depending on the location and type of injury, it is possible that a single implant would be required to have surfaces of all three types (fractured, periosteal, articular). A custom manufactured implant would need to have a rough surface corresponding to the fracture location of the host bone, along with surfaces that allow for continuation of the articular and periosteal regions.

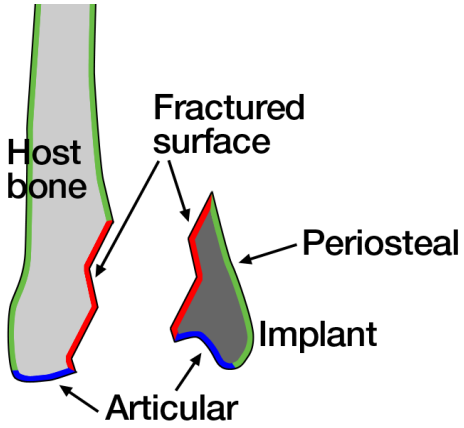

Figure 3.1.3: Different types of implant surfaces

The unique nature of bone injuries between different patients means that orthopedic implants can be widely varied in shape and surface finish requirements.

This often requires an orthopedic surgeon to handcraft a custom implant to suit a particular patient's injury site. During the operation, the surgeon will often make small adjustments to the shape of the implant, compare it with the planned implant site, and then iterate this process until a nominal fit is achieved. In order to reduce some of the uncertainty and inaccuracies in this process, and to help reduce the invasiveness of the surgical procedure, it would be beneficial to manufacture the implants according to medical imaging data obtained from the patient [21]. Previous research has also demonstrated that implants that provide a more stable and accurate fit allow for better healing and patient recovery [5]. Highly accurate 3-dimensional (3D) models of the patient's implant can be constructed from medical imaging data, such as that achieved through computed-tomography (CT) data. To create a more effective implant, a machine is needed that would be able to quickly and easily manufacture the implant according to the 3D model.

The challenge in manufacturing these implants is in development of a process that allows for the creation of highly customized parts with varying surface roughness in select locations. One of the goals of this research is to enable custom bone implants to be manufactured using an automated, push-button process that eliminates the need for the pre-process engineering and skill required to produce the part by conventional manufacturing methods. These requirements have lead to the interest of using layer-based rapid processes in implant manufacturing, which would allow for producing an implant directly from CAD data. Moreover, it is hoped that a computer-aided manufacturing process, utilizing accurate CT derived models, would be able to improve

the accuracy of fit and function for the resulting implant, as compared to handcrafting in surgery. A current research effort at Iowa State University is developing a subtractive RP technology called CNC-RP [24], which is being further developed for manufacturing custom bone implants.

3.1.2 Overview of CNC-RP

Computer numerical control rapid prototyping (CNC-RP) is a subtractive process that combines the automated process planning of RP technology with the capabilities of 4-axis CNC milling to create parts from CAD models. In contrast with additive RP technologies such as FDM or stereolithography, CNC-RP allows for the use of many new materials that can be acquired in stock form, including FDA-approved biomaterials like natural coral, titanium foam, and biocompatible polymers. CNC-RP utilizes a layer-based computer algorithm that analyzes the geometry of the CAD model and finds which part surfaces are visible from different orientations. Beginning with material in round stock form in a 4^{th} axis rotary indexer, the CNC mill machines all surfaces that are visible from a particular setup orientation, after which the indexer rotates the work piece to a new position, allowing the cutting tool to access surfaces that were inaccessible during the previous orientation (Figure 3.1.2.1). This process is repeated until all surfaces of the CAD model have been machined, with the desired part geometry remaining. The automated setup planning algorithm chooses the orientations that allow for complete coverage of the part, while reducing the total number of required rotations [22].

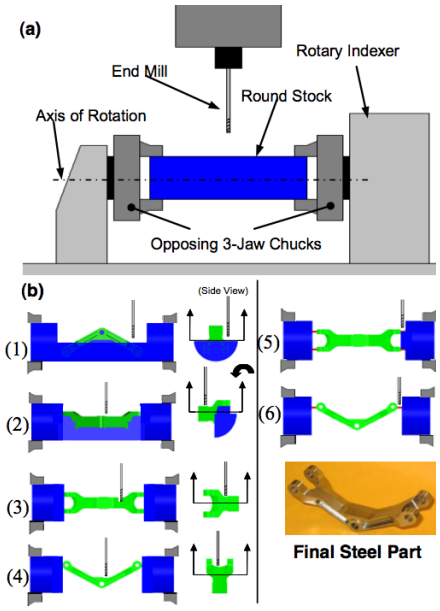

Figure 3.1.2.1: Steel part machined from four different orientations.

Previous research has shown that CNC-RP is effective for producing functional industrial components—parts that have been traditionally cast or machined from steel or aluminum. The resulting parts have good dimensional accuracy and strength, allowing for the creation of functional replacements for parts that have broken down. While the results have been positive when producing industrial parts with CNC-RP, new challenges arise when using it to manufacture orthopedic implants.

The process planning algorithm of CNC-RP examines triangular mesh models of the parts being manufactured, commonly in the STL file format. The triangular facets of the model represent the shape and dimensions of the part. The objective is to ensure that all points of the model that are visible from a particular orientation have been machined. To assess the visibility of a point from a specific orientation, the CAD model is sliced into two-dimensional cross sections, after which the points of each cross section are tested for visibility. During the slicing and visibility test, all points and facets of the model are assumed to represent the same material and surface properties, with the desired result being a manufactured part that has the same shape and dimensions as the model.

In manufacturing orthopedic implants, there is not only the need for replicating the shape and dimensions of the model, but also selective customization of the surface finish of the material. In this case, all points on the CAD model cannot be assumed to have the same properties, requiring a method of customizing the surface properties within select regions of the part. The CNC-RP process needs to target specific surface regions within each orientation, while taking steps to avoid surrounding regions of different surface properties that should not be interfered with. For example, when machining the fractured surface of a bone implant, it is important to make sure the cutting tool stays within the appropriate region, and does not inadvertently touch nearby joint surfaces.

3.1.3 Using CNC-RP for Selective Surface Customization

Expanding on the capability of CNC-RP, Joshi [19] developed methods for targeting custom surfaces using the process. In Joshi's work, polygonal CAD files in the PLY file format were used for process planning. The PLY files contain the definition of triangular facets that have associated color information for representing different types of surfaces. Facets that are red represent the fractured surface, green is periosteal, and blue is the articular surface. The model is sliced into cross sections (Figure 3.1.3.1), with each segment of the slice assigned a color corresponding to the type of implant surface at that particular location. The points on each slice are tested

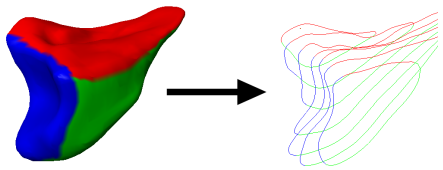

Figure 3.1.3.1: Colored model, and cross sectional slices.

for visibility from different orientation angles. An objective function is used with the goal of choosing setup angles that isolate the different types of surfaces (different colored points of the slices), while also providing full coverage of the part geometry. In Figure 3.1.3.2a, the machining angles generated from the previous method are shown, in which all surfaces of the part are assumed to be the same. Figure 3.1.3.2b shows the setup angles found using Joshi's method, which creates setup angles that better isolate the different surfaces of the part.

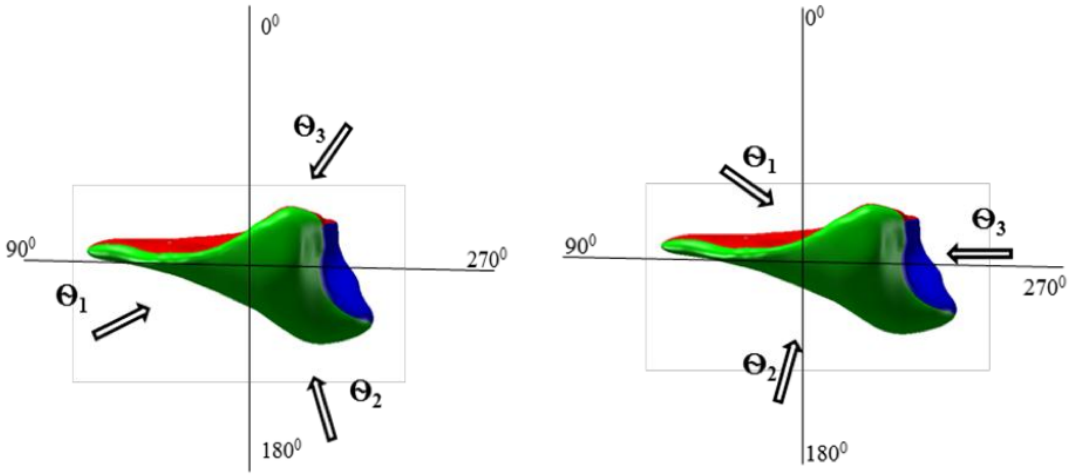

Figure 3.1.3.2: a) Machining setup angles preventing surface customization. b) Setup angles that allow for surface customization by isolating different implant surfaces.

Limitations were noted in cases where the surfaces could not be completely isolated from one another. A setup orientation that was meant for machining only the articular surface would overlap with geometry of a fracture surface, causing the fracture surface to be machined partially. This problem is referred to as *tool path cross over* (Figure 3.1.3.3). This is a problem because inadvertent machining of different nearby surfaces can reduce the effectiveness of the orthopedic implant. For example, if

a surface that is meant to have a rough finish is inadvertently machined smooth by tool paths that cross over into this area, it could reduce the friction at the bone-implant interface, which has a negative effect on implant stability and patient healing.

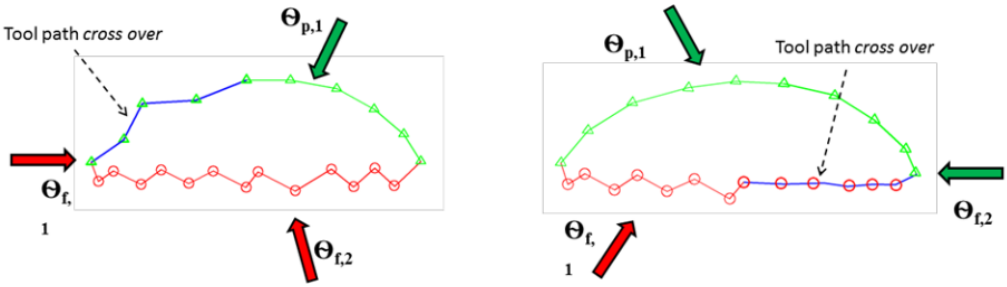

Figure 3.1.3.3: Tool path cross over. a) Tool paths meant for only the green (periosteal) surface will overlap onto the blue (articular) surface. b) Tool paths will overlap from red (fractured) surface onto blue (articular) surface.

3.2 Related Work

Extensive research has been performed in developing the materials and manufacturing methods used for creating effective bone implants. Materials used in bone implants need to be biocompatible, and thus implants are commonly made from materials such as titanium, tantalum, stainless steel, polymethylmethacrylate (PMMA, also referred to as bone cement), and various other biocompatible polymers and ceramics. Considering the unique, free-form shape of biomedical implants, and the desire to create custom implants, many layer-based additive manufacturing methods have been utilized [2, 3, 13, 25]. These methods include fused deposition modeling (FDM), 3D printing, stereolithography, electron beam melting, and laser engineered net shaping (LENS). Melchels et al. [2] evaluated the effectiveness of stereolithography in biomedical applications, and demonstrated that bone implants could be created that

were useful in surgery planning. They also noted that stereolithography had uses in many other biomedical applications such as tissue engineering scaffolding and custom hearing aids. Espalin et al. [3] demonstrated the effectiveness of using FDM to create craniofacial implants out of medical-grade PMMA while approximating the original tissue densities and porosity. A femur model was also fabricated. While the form and fit of the fabricated models were effective, it was noted that the strength of the models could be negatively impacted depending on build direction and porosity.

In bone implant surgeries, a primary concern is the fixation stability of the implant, and the ability for the surrounding bone tissue to react positively with the implant material [17]. An effective bone implant will allow for osseointegration, meaning that living bone tissue grows directly on and around the implant [1, 18], integrating the implant as a permanent part of the patient's body. Research has been demonstrated on the effect of surface properties in orthopedic implants and dental implants on osseointegration, in both humans and animals [6-11]. It was shown that implants made with rough, porous surfaces located at the bone-implant interface are highly effective at aiding osseointegration and bone ingrowth. Titanium dental implants that had been roughened using grit-blasting, acid-etching, or anodizing had significantly higher rates of bone ingrowth and stability than those left untreated [6, 9, 10]. Trabecular metal (a type of metal foam) has been utilized in bone implant research because it provides pores for bone tissue to grow into. Deglurkar et al. [7] demonstrated that when trabecular metal implants were machined, the pores were smeared and closed, resulting in less bone ingrowth and a less effective implant.

Research has been performed regarding methods for machining trabecular metal without smearing and closing the pores [4]. Using an infiltrant, the smearing was greatly reduced during machining, and the pores were preserved. It was proposed that the infiltrant could also act as a barrier that prevents contaminants from entering the implant during manufacturing.

In total hip replacement surgery, the majority of implants are fixated without the use of bone cement [20]. Early research by Albrektsson et al. [14] showed evidence that osseointegration could occur in humans without the use of cement, using threaded titanium screws. Tight initial fixation stability was noted as a primary requirement for ensuring permanent osseointegration, and preventing tissue irritations at the implant interface [5, 14, 15]. It has been estimated that around 5-10% of hip replacements fail within the first 10 years, and it has been shown that micromotions at the bone-implant interface are a primary cause [13]. Micromotions are microscopic movements between the implant and bone surface. These motions are often difficult to detect, and can lead to loosening of the implant over the long term. In order to maintain high initial fixation, and a reduction in motion at the bone-implant interface, a high amount of friction is desirable at the interface [12, 16]. Hsu et al. [16] demonstrated that micromotion increased as friction between the implant and bone surfaces decreased. It was shown that an implant surface with a coefficient of friction of 0.5 or above could reduce the motions by over 20%, which lead to an increase in bone ingrowth.

3.3 Overview of Proposed Methods

This paper proposes new methods that allow us to provide customized surface characteristics in rapid machining patient-specific bone implants. It addresses two basic objectives: 1) How can one more accurately provide slice data for initial setup planning and 2) Given a set of setup angles, how can one ensure that the individual surfaces are machined independently? In doing so, this work considers the overarching problem of ensuring that the biocompatibility of the implant is maintained and optimized. For the first problem, providing accurate slice information, this thesis presents a method of modifying the initial slice data if ambiguous surface boundaries are found (uncertainty in the form of "noise", with respect to boundary type). To address the second problem, ensuring surfaces are independently machined, this work presents a method for creating tool path containment boundaries that restrict the tool from machining neighboring surfaces. A tool containment boundary is a feature found in some computer-aided manufacturing (CAM) software packages that can be used for constraining the cutting tool to a particular region of the part. This allows the user to draw a polygonal boundary that defines where the cutting tool should or should not cut, which is a manual, rather than rapid procedure. In Figure 3.3.1a, a simulated piece of stock material is shown before machining. Figure 3.3.1b shows the part after machining every visible surface from this particular setup. A rectangular tool containment boundary was then drawn over the top of the part, and the machining was simulated again (Figure 3.3.1c). The cutting tool stayed within the rectangular tool

containment boundary, allowing some of the stock material surrounding the part to remain.

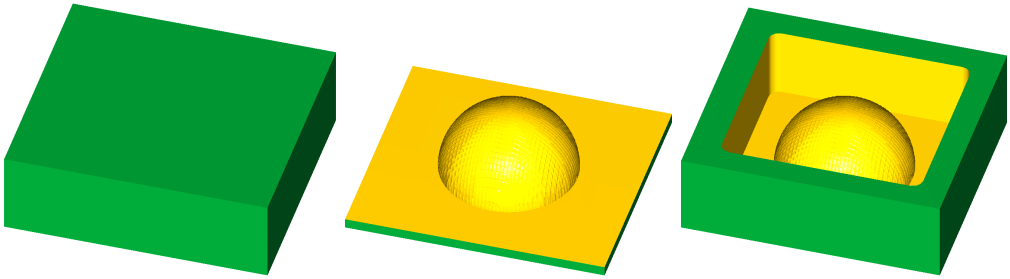

(a) (b) (c)

Figure 3.3.1: a) Stock material before machining. b) Stock is machined to reveal a part, without tool containment boundary. c) A rectangular tool containment boundary is used to allow some of the original stock surrounding the part to remain.

In both methods, the issue of biocompatibility is actively addressed by sequentially giving priorities to the 3 major surfaces where modifications to the slices, or boundaries for tool paths are chosen based on the type of surface it is modifying. Throughout the remainder of this paper, the fracture, periosteal, and articular surfaces will be represented by the colors red, green, and blue respectively. In some figures, the different types of surfaces will also be represented by the following symbols: ○ for fracture surface, △ for periosteal, and □ for articular.

3.4 Slice Modification

Several factors can lead to ambiguous or inaccurate material boundaries in both the CAD model and the manufactured part. Defining appropriate surface boundary lines requires overcoming limitations in the resolution of the triangular mesh model and in dimensional control of the manufactured part. Coloring the facets of a triangular mesh model (Figure 3.4.1) can lead to fragmented saw-tooth-like boundaries between

regions of differing color. In Figure 3.4.2, triangular facets are shown at the boundary between a fracture and periosteal surface, with a dark line in the middle representing a slice that is cut through that region. The facets that lie directly underneath the slice alternate between fracture (red), and periosteal (green).

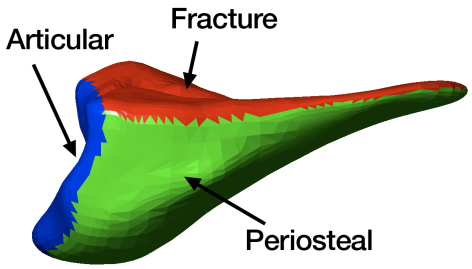

Figure 3.4.1: Colored triangular mesh model of implant, showing articular (blue), periosteal (green), and fracture (red) surfaces.

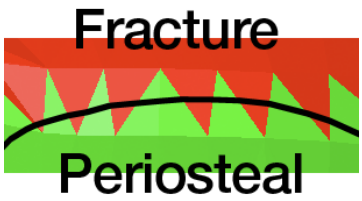

Figure 3.4.2: Fragmented boundary between fracture and periosteal surfaces. A partial slice is shown as a dark line cutting through the jagged area.

These fragmented boundaries arise from limitations in the resolution of the mesh, and are ambiguous in that they do not represent the true boundary that would occur naturally in the bone.

When slicing (Figure 3.4.3) the model for visibility analysis, slices that lie across a rough boundary will contain a series of small segments that alternate back and forth between colors, as did the facets that the slice segments originate from. These small segments can have an undesirable influence on the evaluation of setup angles for the model. In this paper, such problem segments that arise from

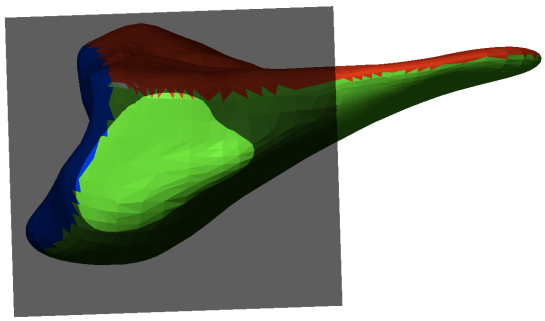

Figure 3.4.3: Slice plane intersecting implant model.

ambiguous surface boundaries will be referred to as *noise segments* and such slices will be considered noisy (Figure 3.4.4b).

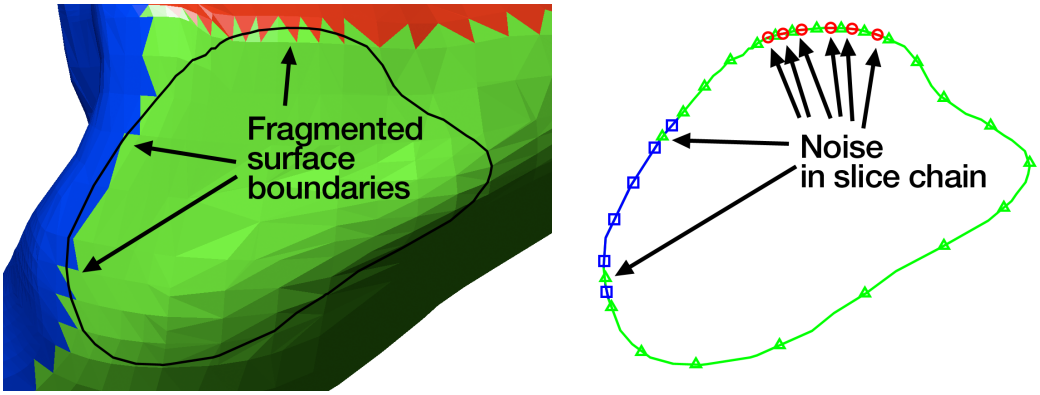

(a) (b)

Figure 3.4.4: a) Close view of intersection of slice plane and implant model, showing areas where the slice crosses rough surface boundaries. b) Colored slice, with color information originating from the colored facets of the corresponding area of the model. Noise has been produced by crossing through rough surface boundaries.

Noise occurs at the edges of different surfaces, and can cause the setup angle solution to be skewed in different directions, because the method for finding setup angles will try to include the noise in the solution even if it is unimportant relative to the main body of the surface. A simple example is shown in Figure 3.4.5a. A slice containing two different colors is shown with a direction arrow showing the direction of visibility (setup angles) for each of the two colors. The slice in Figure 3.4.5a contains small, fragmented segments (noise) on the left side, causing setup angle 2 to shift around slightly to the left in order to include those small segments. In Figure 3.4.5b, the noise segments have been removed, allowing setup angle 2 to shift down and to the right, more in line with the large continuous slice segment, because it no longer needs to include the small segments in its visible area.

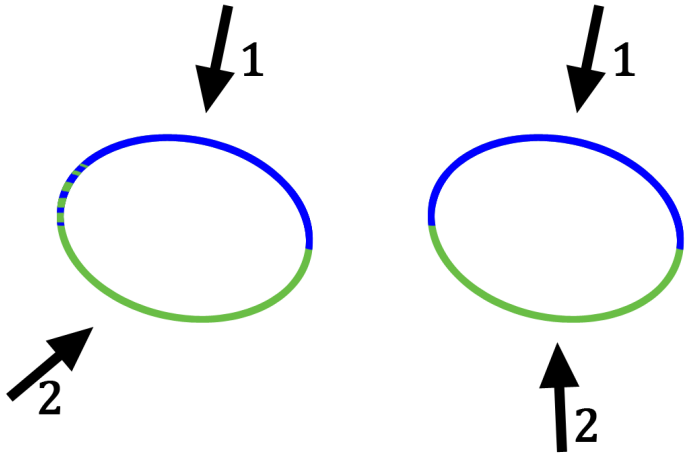

(a) (b)

Figure 3.4.5: a) Slice has small noise segments on the left side. b) After removing the noise segments, setup angle 2 shifts downward and to the right.

Slices will be modified using a method to remove noise segments that will help prevent ambiguous surface boundaries from negatively influencing the setup orientation solution. To ensure that biocompatibility is maintained, the noisy segments will be modified and potentially assign a new color according to the relative priorities of the surfaces in question. With regard to biocompatibility, articular surfaces take priority over periosteal surfaces, and periosteal surfaces take priority over fracture surfaces. A simple overview of the slice modification process is shown for a single slice in Figure 3.4.6. Starting at an initial point on the slice, the segments are searched through by traveling counterclockwise around the slice, identifying and removing small segments of color that interrupt large sections of the chain.

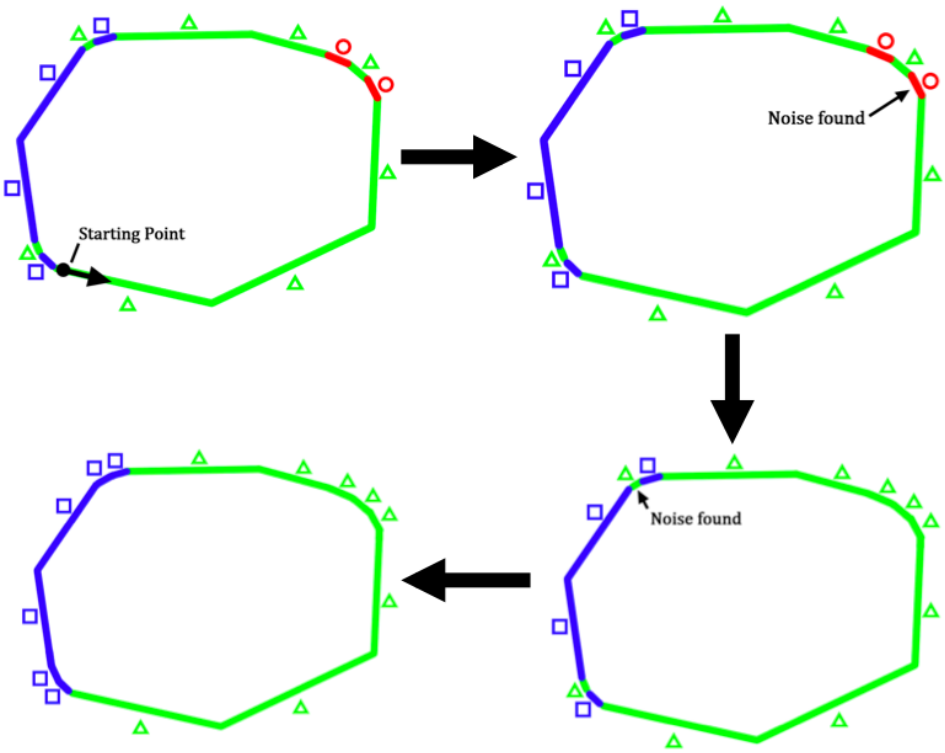

Figure 3.4.6: Starting with the initial slice data (upper left), the algorithm searches for noise segments while traveling counter-clockwise along the slice, resulting in a clean slice with noise segments removed (lower left).

To facilitate the discussion of the proposed method for slice modification for colored bone models, the following is defined:

T : $\{T_1, T_2, \ldots, T_n\}$	Set T of n triangles, each denoted T_i, is the set of colored triangular facets that comprise the bone implant model. Each facet is assigned a color red, green, or blue corresponding to the type of surface.
S : $\{S_1, S_2, \ldots, S_n\}$	Set S of n slices, each denoted S_i, is the colored slices obtained from intersecting the model with slice planes.
C : $\{C_{i1}, C_{i2}, \ldots, C_{im}\}$	Set C of m chains in a slice, each denoted C_{ij}, where C_{ij} is the j^{th} chain of the i^{th} slice.
P : $\{P_{ij1}, P_{ij2}, \ldots, P_{ijp}\}$	Set P of p points in a chain, each denoted P_{ijk}, where P_{ijk} is the k^{th} point of the j^{th} chain of the i^{th} slice.
L : $\{L_{ij1}, L_{ij2}, \ldots, L_{ijp-1}\}$	Set of line segments that comprise a slice chain. L_{ijq}

	denotes the line segment connecting points P_{ijk} and P_{ijk+1} in a chain. Each line segment is assigned a color red, green or blue depending on the surface it originates from.
l_{min}	If an isolated group of line segments of the same color has a total length less than l_{min}, the segments are considered to be noise.
$Color_c$	The color (red, green or blue) of the most recent series of segments that have been deemed not noise.
$Color_n$	The color (red, green or blue) of a segment that has been found to interrupt the continuation of a sequence of non-noise segments.
$\mathbf{G} \subseteq \mathbf{C}$	Set G is the current set of line segments found to interrupt the continuation of non-noise segments, which will be evaluated to decide whether or not the set is noise, or is data that should be kept in its current form. G will either be empty, or refer to a subset of C.

A slice chain is comprised of a set of points that are specified in either clockwise or counterclockwise order. The first step of the noise removal process is to search through the chain to find a starting point that lies in an area that is known to not be noise, so the chain is searched to find the largest uninterrupted section of a single color. $Color_c$ is initialized to the color of the largest section, and the starting point is chosen to be at the beginning of this section (Figure 3.4.7 Starting point). With the starting point lying on a large, unbroken section of the chain, it is assumed that the noise removal process begins on a part of the chain that is not noise.

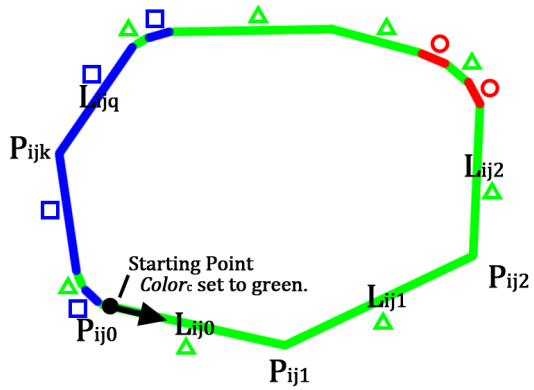

Figure 3.4.7: Starting point of slice.

When searching through the remainder of the chain, if a line segment is found to have a color differing from $Color_c$, the new color is referred to as $Color_n$. Segments further down the chain will be examined (traveling counter-clockwise around the chain) to determine if the segment(s) of $Color_n$ represent a new surface region or noise. Depending on what is found after the change to $Color_n$, the new segments may or may not be assigned a different color depending on rules that are proposed for the relationship between $Color_c$ and $Color_n$. In other words, if a section of an articular surface is being traversed, it needs to be determined where the surface actually begins and ends. If new segments are found that suddenly interrupt the articular surface, they will be further examined to determine if the real boundary of the surface has been found, or if the new segments are just a result of noise in the slice data.

Set G is initially empty at the beginning of the noise removal process. When a color differing from $Color_c$ is found, the new segment is added to G (Figure 3.4.8). In the example in Figure 3.X (First red), a fracture (red,) is added to G, and $Color_n$ is set to red.

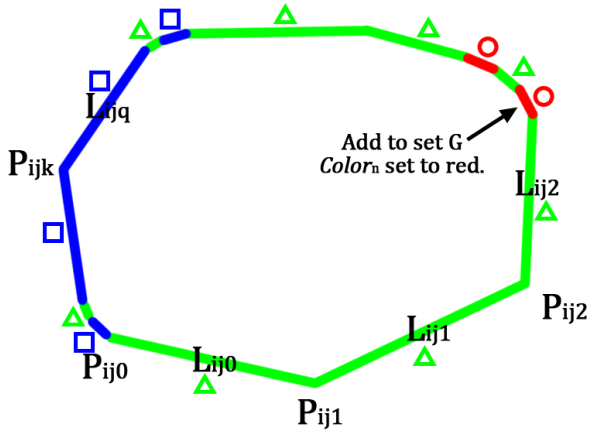

Figure 3.4.8: Fracture (red) segment found.

If subsequent segments of the new color ($Color_n$) are found, they will also be added to G. Subsequent line segments are examined until one of three events happen: 1) A new segment is found that is the same as the original color ($Color_c$), 2) The total length of segments in G is found to be greater than or equal to l_{min}, or 3) A new articular (blue,) segment is found.

In scenario 1, a chain of color has been found that is interrupted by some set of segments in G. If $\sum(length\ of\ G_i) < l_{min}$, the segments of G themselves do not comprise a section long enough to be considered a "good" surface region, and must be examined by color to decide how the noise will be handled. In the slice shown in Figure 3.4.9, a periosteal (green,) segment is found after a fracture (red,) segment was added to set G. The fracture (red,) segment in G does not meet the minimum length l_{min}, so it is changed to green ( ) to allow the periosteal section to continue without interruption, and set G is emptied. This is done because $Color_c$ is currently tracking periosteal segments, which have a higher priority than fracture segments, which is what was represented by $Color_n$.

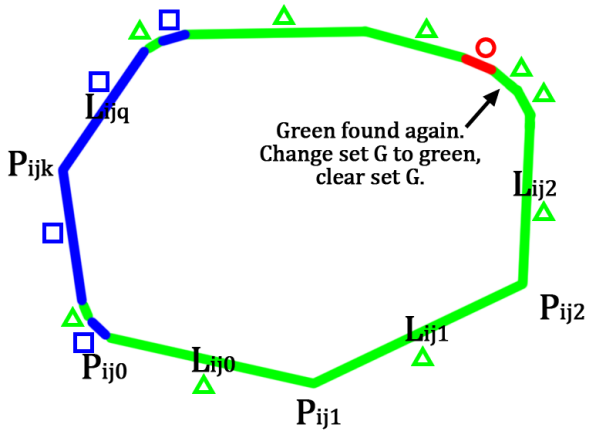

Figure 3.4.9: Periosteal (green) segment found immediately after red. Previous red segment changed to green.

Continuing the counter-clockwise search around the chain, another fracture (red, O) segment is found, added to G, and $Color_n$ is again set to red. Another periosteal (green, △) segment is found next. Since the segment in G is less than l_{min}, and $Color_c$ (green) has a higher priority than $Color_n$ (red), the segment in set G is changed to green, allowing the periosteal (green, △) segments to continue on without interruption.

In scenario 2, $\sum(length\ of\ G_i) \geq l_{min}$ means that set G is a long continuous section that is considered to be part of a "good" surface (not noise). In this case, $Color_c$ is assigned the color of this section, and the search then continues throughout the remainder of the chain until another event occurs. In the example slice shown in the previous figures, if the fracture (red, O) segments that were added to set G had met the minimum length requirement, the red segments would have been allowed to stay and "red" would have been the new value of $Color_c$.

In scenario 3, an articular (blue,) segment has been found, therefore $Color_c$ is immediately assigned blue, and the process continues on the remainder of the chain assuming a "good" blue section is present. Since blue segments represent articular surfaces, which are critical to maintaining biocompatibility, they are always assumed to be non-noise and will not be removed from the chain. Blue segments are handled in this manner to ensure that an articular surface will not be reduced in size, which helps ensure that a joint between bones will not be damaged.

In Figure 3.4.10, an articular (blue,) segment is found. This follows scenario 3, so "blue" will be the new value of $Color_c$. Next, a periosteal (green,) segment is found, so $Color_n$ is set to "green", and the segment is added to G. Another articular (blue,) is found next, so the length of the segment in G is examined. The length of the periosteal segment in G is less than l_{min}, so it will be changed to blue to allow the articular segments to continue without interruption. The same happens with the last small periosteal segment that interrupts the articular section. It is found to have a length less than l_{min}, so it is changed to blue to allow the articular segments to continue without interruption, leaving the final slice as shown in Figure 3.4.11.

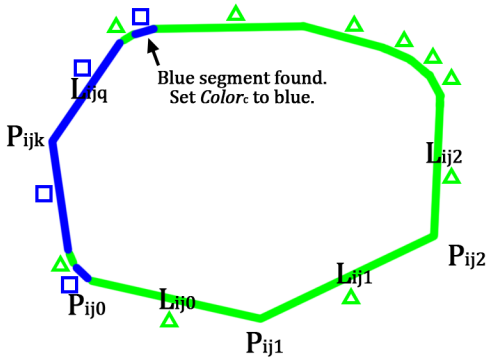

Figure 3.4.10: Articular (blue) segment found.

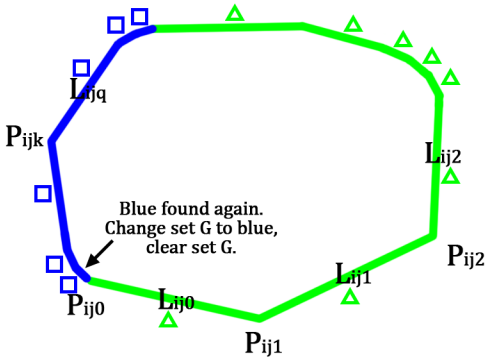

Figure 3.4.11: Final noise segment changed to blue, all noise removed.

Table 3.4.1: Rules for modifying colors of slice segments based on relative priority of surface types of $Color_c$ and $Color_n$

$Color_c$	$Color_n$	Resulting effect on segments in G
Blue (articular, □)	Red (fracture, ○)	Change to blue.
Blue (articular, □)	Green (periosteal, △)	Change to blue.
Green (periosteal, △)	Red (fracture, ○)	Change to green.
Green (periosteal, △)	Blue (articular, □)	Change to blue.
Red (fracture, ○)	Blue (articular, □)	Change to blue.
Red (fracture, ○)	Green (periosteal, △)	Change to green.

This process is repeated for every chain in C for every slice in S. The slice modification process results in the set of improved slices S'. To obtain machining setup angles, S' is analyzed for visibility and set coverage using existing methods. The slice modification and visibility analysis processes allow for the cutting tool to be aimed in the general direction of the surface, but it is still possible for multiple surfaces to be visible from the same angle (Figure 3.4.12). In the example in Figure 3.4.12, tool paths meant for the articular surface would also machine the other surfaces that are visible from this orientation, which leads to a reduction in the ability to customize the surface

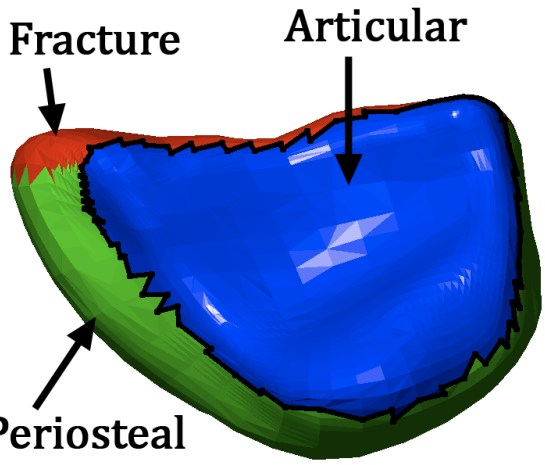

Figure 3.4.12: Three different surfaces visible from one orientation.

characteristics of the implant. A method is needed for constraining the tool to a particular surface in a way that does not allow it to interfere with neighboring surfaces that are also visible from that setup angle. This problem is addressed in the next section by constructing tool path containment boundaries specific to each type of surface.

3.5 Generating Tool Path Containment Boundaries

The second research question proposed at the beginning of this paper was how can one ensure that the individual surfaces are machined independently? To address this issue, a method for constructing tool path containment boundaries is proposed. To construct a containment boundary, one must first determine which areas of an implant surface are visible from each setup angle. With visibility information available from the slices of the model, it is possible to determine which facets of the CAD model are visible from a particular setup orientation. Coupled with the color information of each facet, it is possible to determine exactly which regions of the visible surface correspond to each type of implant surface (articular, periosteal, or fracture). For example, in using the visibility and color data, a method can be developed for identifying the facets of the articular surface from Figure 3.4.12. If a polygon can be traced along the outer

boundary of the articular surface, it will be possible to constrain CNC tool paths to this surface, preventing the tool from cutting the neighboring fracture and periosteal surfaces. In the following, a method for constructing the boundary polygon is presented.

The slices from S', setup angles and visibility results are used for determining which facets of the 3D model are visible from a particular setup angle. The set of visible facets for a particular surface type are projected onto the tool plane, and then a Boolean union operation is performed on the projected facets to create an irregular polygon outlining the boundary of the surface (Figure 3.5.2).

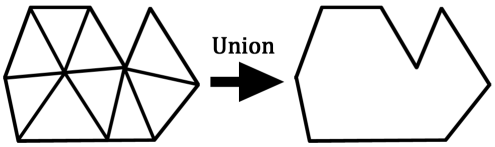

Figure 3.5.1: Boolean union of triangles, resulting in a single polygon.

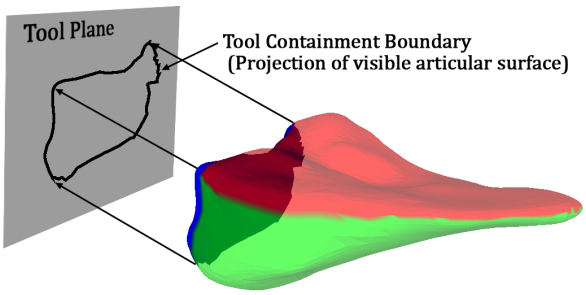

Figure 3.5.2: Surface projected onto tool plane.

The visibility algorithm returns the set of required machining angles. To construct a tool path containment boundary for a particular machining angle, the points of each slice in set S are examined to find which points are visible from that machining angle. If a point of a slice is found to be visible, the triangular facet that it is mapped to will be inspected to determine if it is of the color of interest (blue for articular, green for periosteal, red for fracture). If it is the desired color, the triangle will be projected onto

the tool plane that has been constructed for this machining angle, giving a new triangle t', which is added to set T'.

For $(S_i, i = 1 \dots n)$
    For $(C_{ij}, j = 1 \dots m)$
        For $(P_{ijk}, k = 1 \dots p)$

            If P_{ijk} is visible from plane.angle
                Get triangle t from T mapped from Pijk

                If t matches color of interest
                    Project t onto plane to get t'
                    Add t' to T'

Figure 3.5.3: Gathering the set of visible facets for containment boundary

After collecting the visible triangles of the desired color, a new polygon is formed by computing the 2D Boolean union of all elements of T'.

For $(T'_i,\ i = 1 \dots n)$
    $B = B \cup T'_i$

Figure 3.5.4: Construct containment polygon B from set T'

Given the nature of the triangular mesh model, these polygonal boundaries can have very jagged and irregular edges, which do not accurately reflect the "true" surface boundary (Figure 3.5.5a). The more desirable boundary, with jagged areas smoothed out, is shown in Figure 3.5.5b.

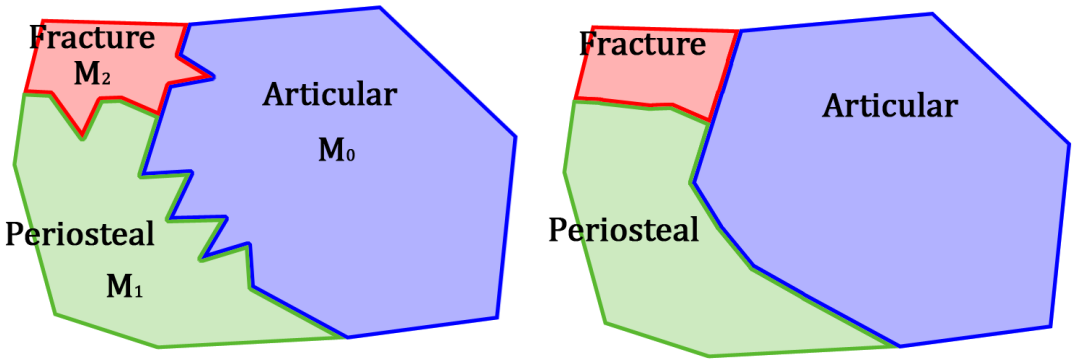

(a) (b)

Figure 3.5.5: a) Initial jagged containment boundaries. b) Smoother, more desirable containment boundaries.

To compensate for this, a polygon smoothing process has been developed that will reduce jagged edges in a way that maintains biocompatibility by assigning priority to the different types of surfaces. It is worth noting that many different polygon smoothing algorithms exist, and most rely on subdividing the line segments of the polygon or fitting a curve to the vertices. Chaikin [26] developed an approximating algorithm for subdividing and smoothing polygons. Since the data points are approximated, the resulting curve will lie inside or outside of the original polygon in certain areas, resulting in a loss of surface area in some regions, and an increase in area in other regions, which would violate the rules of surface priority previously stated in this paper. Dyn et al. [27] developed a similar algorithm that interpolates the original data points of the polygon, but still results in the same issues of gaining or losing polygon surface area in areas that would be undesirable based on concerns of biosensitivity of the implant surfaces. Piegl and Tiller [28] discuss methods for fitting data points with NURBS curves, but it is noted that there are infinitely many NURBS curves that can be fit to a given set of data points, and the curve will travel both inside

and outside of the original polygon in a ways that are difficult to control. To address the problems of biosensitivity of the implant surfaces, and the desire to only increase or decrease the area of the polygon based on relative priorities of the surfaces (for example, it may be desirable to always increase the size of an articular surface, but not a fracture surface, to prevent possible damage to joint tissue), a different approach has been taken in this research.

Consecutive points along the polygon chain are examined to find sharp spikes, and depending on the priority of the surface in question relative to surrounding surfaces, points may be translated in a way that would help eliminate the spike. It has been found that tool containment boundaries will have sharp spikes that are either inward pointing or outward pointing (Figure 3.5.6). Inward pointing spikes occur when a facet of a differing surface type lies across the "true" surface boundary, meaning that the tool containment boundary is possibly smaller than it should be. Outward pointing spikes occur when a facet of a surface lies across the "true" boundary of that surface type, meaning it is possible that the surface is possibly larger than it should be.

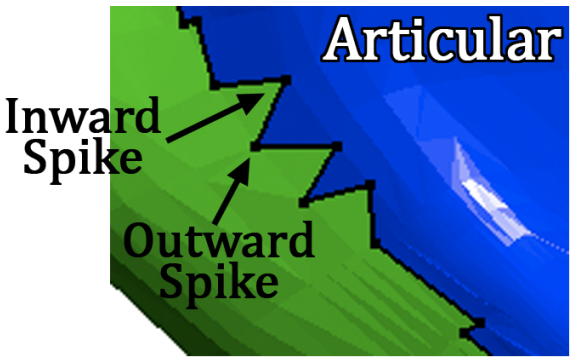

Figure 3.5.6: Sharp spikes in boundary.

For example, if a tool containment boundary for an articular surface is found to have an inward pointing spike that protrudes into the articular boundary, the tip of the spike will be moved outward to eliminate the spike and enlarge the articular surface

slightly. This is done to create a smoother boundary that would mimic the "true" surface boundary, and biocompatibility is preserved by ensuring that the articular surface will never be reduced in size. In the case of a periosteal boundary, the tip of an inward pointing spike will only be allowed to move outward if it is found to lie across the boundary of a fractured surface, and will not be moved outward if found to impede on an articular surface. This allows for smoothing of the periosteal boundary, and preserves biocompatibility by ensuring that an articular boundary will not be reduced in size.

Since multiple implant surfaces can be visible from a particular machining angle, there will be multiple tool containment boundaries constructed for each machining angle, each targeting a specific type of surface. Let M represent the set of tool containment boundaries for a particular machining angle, with each individual boundary denoted M_i. Each tool containment boundary M_i is a polygonal chain comprised of a number of points, each denoted M_{ij}, which represents the jth point of the ith tool containment boundary polygon. The method for smoothing the tool containment boundary begins with a polygonal chain M_i, which represents the tool containment boundary that has been constructed from the Boolean union of the facets of a particular implant surface that have been projected onto the tool plane.

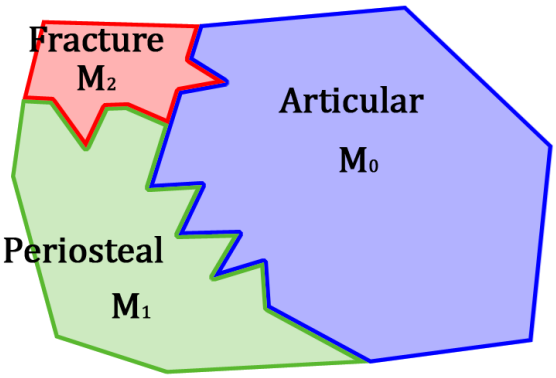

Figure 3.5.7: Multiple tool containment boundaries constructed on the tool plane from the same setup orientation.

For each group of three consecutive points within M_i, denoted $M_{i,j}$, $M_{i,j+1}$, and $M_{i,j+2}$, two vectors $\vec{v}_a$ and $\vec{v}_b$ are constructed:

$$\vec{v}_a = M_{i,j+1} - M_{i,j}$$
$$\vec{v}_b = M_{i,j+2} - M_{i,j+1}$$

The two vectors are then normalized so they are each of unit length. $\vec{v}_a$ and $\vec{v}_b$ represent the directions of the two edges connected to point $M_{i,j+1}$. To determine if point $M_{i,j+1}$ comprises the point of a spike, the two edge vectors are compared to determine if an extreme angle is formed. This is computed using the dot product $\vec{v}_a \cdot \vec{v}_b$. If the dot product is less than D_{min}, it is concluded that a sharp spike is present. In practice, it has been found that 0.4 is a good value for D_{min}, which means that an angle of approximately 66 degrees or less between edges is considered "smooth", and an angle greater than that will be considered a sharp spike. A simplified example is shown in Figure 3.5.8, where spikes are eliminated step by step by comparing angles between

adjacent pairs of edges and eliminating the tip of the spike if found to meet the angle threshold.

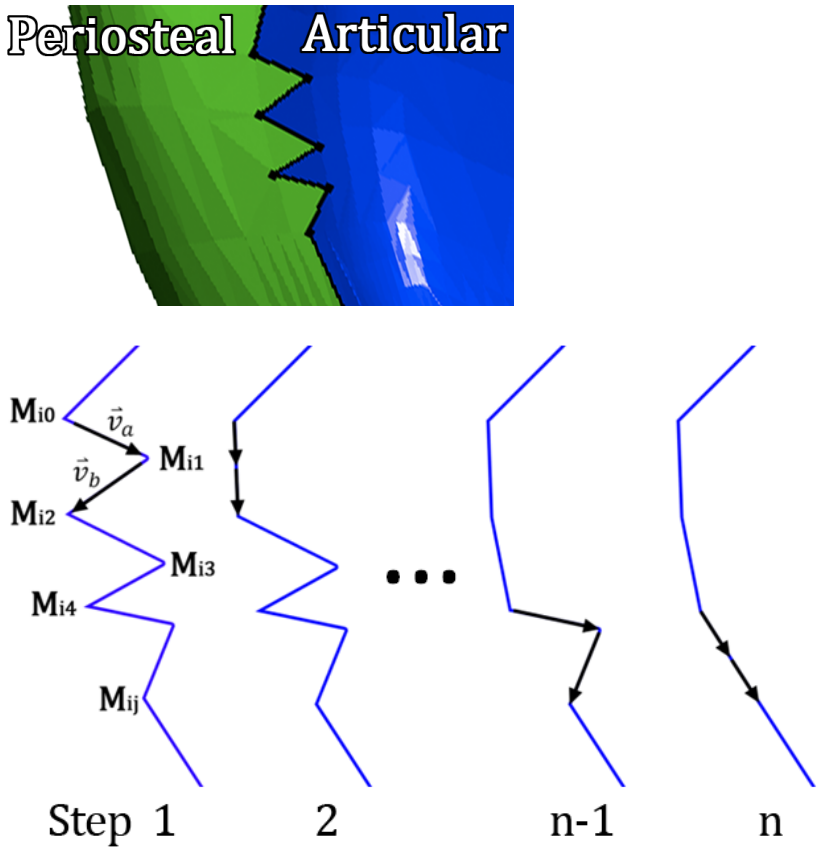

Figure 3.5.8: A jagged boundary between an articular and periosteal surface (left) is smoothed by comparing the angle between adjacent edges along the chain, with the final smooth boundary shown on the right.

If the value of the dot product is less than D_{min}, then a sharp spike has been found. Depending on the type of implant surface being targeted by M_i, the types of surrounding surfaces that are present, and whether the spike points inward or outward, $M_{i,j+1}$ may be modified to eliminate the spike. Let point $M'_{i,j+1}$ represent the modified position of $M_{i,j+1}$ for eliminating the spike, which is computed as the midpoint between $M_{i,j}$ and $M_{i,j+2}$. To decide if the spike points inward or outward, $\vec{v}_a$ is

examined to determine if it is directed towards the interior of the polygon or away from it. This is found by travelling in the direction of $\vec{v}_a$ from point $M_{i,j+1}$. If the interior of M_i has been entered immediately, then the spike points inward, otherwise the spike points outward.

Once a spike has been identified, the surface type is taken into consideration to help determine how the spike will be handled. Inward and outward pointing spikes are treated differently, and first the method for inward spikes will be examined. If M_i is the boundary for an articular surface, and the spike points inward, $M_{i,j+1}$ will be set to the position of $M'_{i,j+1}$. This eliminates the spike and, since $M_{i,j+1}$ is moved outward, makes the articular region slightly larger. In this case, the surrounding surfaces are not taken into consideration, because articular surfaces always take precedence over the other types of surfaces, so an articular surface will always be made larger regardless of surroundings. If M_i is the boundary of a periosteal surface, $M_{i,j+1}$ will be modified only if $M'_{i,j+1}$ does not intersect an articular boundary. All other boundaries in set M will be examined and if it is found to intersect an articular boundary, $M_{i,j+1}$ will remain unmodified in this scenario. Inward pointing spikes are not modified for fractured surfaces, because fractured surfaces are of the lowest priority and will not be enlarged, which would cause either a periosteal or articular surface to be reduced in size.

If the identified spike points outward, a different set of rules applies for modifying spikes. For outward pointing spikes, moving point $M_{i,j+1}$ to $M'_{i,j+1}$ would bring the point inward toward the interior of the boundary, eliminating the spike and making the bounded region slightly smaller. For an articular boundary, an outward

spike would be ignored, because it is not desirable to reduce the size of an articular surface, as this would have a negative effect on biocompatibility. If an outward spike is identified in a periosteal boundary, point $M_{i,j+1}$ will be moved inward to $M'_{i,j+1}$ if it is found that the spike intrudes on the boundary of an articular surface. This is determined by travelling in the direction of $\vec{v}_a$ from point $M_{i,j+1}$, and performing an intersection test with the other boundaries in set M. If an articular surface boundary is intersected, then the point is moved and the spike is eliminated, otherwise the point will remain unchanged. If M_i is a fractured surface boundary, the outward spike will be eliminated if it is found to intersect with any other surface type, again because the fractured surface is of the lowest priority. In general, fractured surfaces will be made smaller to accommodate for making other surface types larger. The assumption is that reducing the size of a fractured surface, while reducing fixation stability, enables the periosteal and articular surfaces to be enlarged, which is desirable for ensuring biocompatibility.

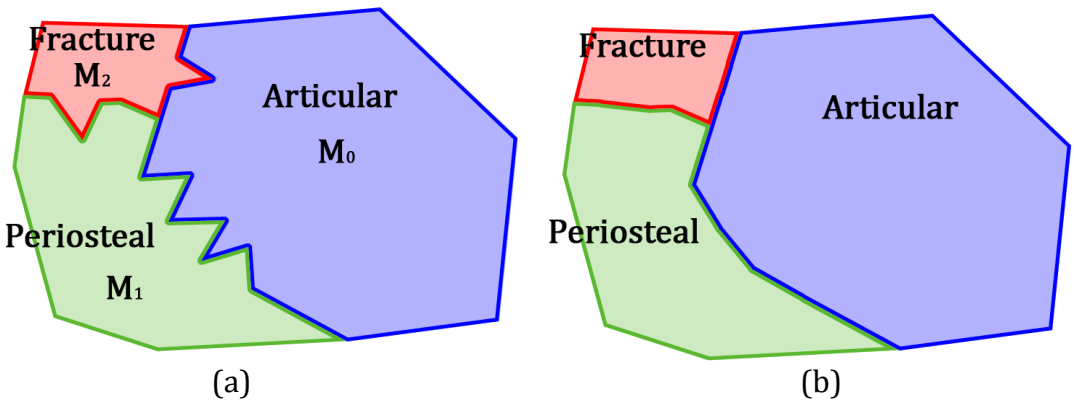

Figure 3.5.9: a) Tool containment boundaries before smoothing. b) Final tool containment boundaries after smoothing is performed.

3.6 Implementation and Results

The proposed methods were implemented in software written in C++, with a graphical interface using OpenGL. The software was tested on a computer with a 2.4 GHz Intel Core 2 Duo processor running Mac OS X version 10.6.6. The program accepts colored 3D models in the Stanford Polygon (PLY) file format, performs slicing, slice modification, visibility analysis, and generates tool containment boundaries based on the slicing and visibility results. Analytical results are also reported for quantifying tool path crossover and redundant machining. The program utilizes the VCG library [29] for reading PLY files, and the Computational Geometry Algorithms Library (CGAL) [30] for performing 2D Boolean set operations.

The VCG I/O and Trimesh modules were used for reading the contents of the PLY files and gathering the facet information. The OpenGL wrapper functions of the VCG library were also used for displaying the PLY model in an OpenGL viewport. The model was then sliced, noise removal was performed, and the improved slices were used for finding the machining angles using previous methods developed by Joshi [19]. Tool containment boundaries were generated as described in the previous section, by projecting visible triangular facets onto the tool plane for the corresponding machining angle. The 2D Polygon and 2D Regularized Boolean Set-Operations packages from the CGAL library were used for performing the Boolean union of the projected facets on the tool plane.

The bone implant models shown in Tables 3.6.1 and 3.6.2 were studied with the program. For each model, the reduction in redundant machining on the model and the

increase in the ability to customize the implant fracture surface is shown. The total length of noise segments removed during the slice modification process is also given. The reduction in redundant machining is the percentage of the total surface area of the model that would have been machined from one setup angle, and then passed over again during a subsequent setup resulting in wasted machine time. The increase in fracture surface customization shows the percentage of the fracture surface that would be cut away and lost with the previous setup planning method, but can now be preserved with the new method. This is presented as one of the primary metrics for maintaining the biocompatibility of the implants, because preserving the fracture surface may allow for increased fixation stability and improved healing time for the patient.

Table 3.6.1: Example bone implants.

	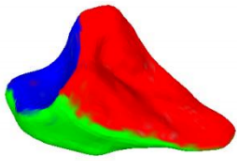 (1)	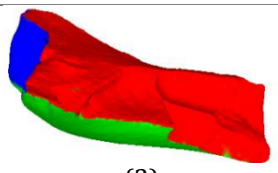 (2)	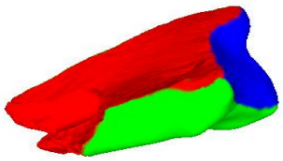 (3)
Noise Removed	12.0 mm	2.7 mm	7.3 mm
Redundant machining reduction	25.8%	23.1%	34.9%
Fracture surface customization increase	7.7%	4.5%	3.4%

	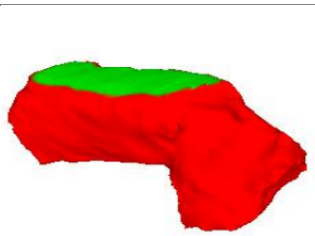 (4)	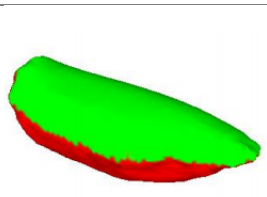 (5)	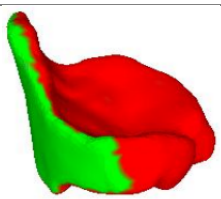 (6)
Noise Removed	0 mm	0 mm	0 mm
Redundant machining reduction	41.2%	0%	4.2%
Fracture surface customization increase	34.2%	0%	4.3%

In Table 3.6.3, a detailed breakdown of the setup angles, tool path cross-over and various other metrics are shown for each step of the process for model 1. The first column of the table (Model 1 Original) shows the setup angles and amount of tool path cross-over for the original setup of model 1 before any improvements were made. There is cross-over from the articular to fracture (A to F) surfaces of 7.7%, meaning that the fracture surface would be reduced by 7.7% while machining from the articular setup orientation, which causes a reduction in initial fixation stability of the implant and has a negative impact on patient healing time. There is also a significant amount of cross-over from the periosteal to articular (P to A) and articular to periosteal (A to P) surfaces: 84.1% and 23.6% respectively, which translates to redundant machining on 25.8% of the total surface area of the model. These cross-over values, while not having a large impact on biocompatibility or fixation stability, result in redundant machining (wasted machine time).

Table 3.6.3: Setup angles and cross-over statistics for model 1.

	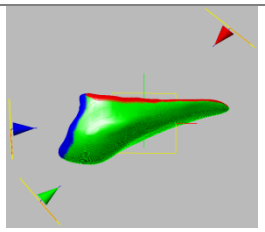	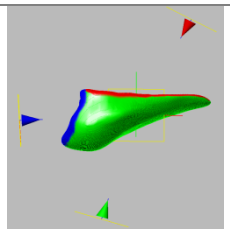	--
	Model 1 Original	Model 1 After Noise Removal	Model 1 With Tool Containment Boundaries
Noise Removed:	--	12.0 mm	--
Articular Angle:	183°	--	--
Periosteal Angle:	219°	253° (+34°)	--
Fracture Angle:	50°	62° (+12°)	--
P to A:	84.1%	33.7% (-50.4%)	0% (-33.7%)
P to F:	1.6%	1.1% (-0.5%)	0% (-1.1%)
A to P:	23.6%	--	0% (-23.6%)
A to F:	7.7%	--	0% (-7.7%)
F to P:	10.5%	10.1% (-0.4%)	0% (-10.1%)
F to A:	4.8%	7.8% (+3.0%)	0% (-7.8%)
Redundant Machining	25.8%	17.8%	0% (-17.8%)
Fracture Surface Improvement	--	--	7.7%

After removing noise segments from the slices of model 1, the results were examined to note improvements in the ability of the setup angles to isolate the different types of surfaces (Table 3.6.3, Model 1 After Noise Removal). Noise removal had a pronounced effect on the setup angle solution, causing a 34° shift in the periosteal setup angle, and a 12° shift in the fracture setup angle. The change in the periosteal setup angle reduced the tool path cross-over from the periosteal to articular (P to A) surfaces by 50.4%. This reduces wasted machine time, since the tool paths for the periosteal surface will no longer repeat over the articular surface in multiple setups. The shift in the fracture setup angle allows the cutting tool to contact the surface at an angle closer

to the surface normal, which allows for the application of a more uniform rough surface texture.

After the shift in setup angles, model 1 still showed tool path cross-over since multiple surfaces were still visible from some setup angles. Tool containment boundaries were then constructed to isolate each type of surface from one another during machining. This causes the remainder of the tool path cross-over to be largely irrelevant (Table 3.6.3, Model 1 With Tool Containment Boundaries). With the use of tool containment boundaries, 7.7% of the fracture surface can be preserved. The 7.7% of the fractured surface is 125.3 mm^2 of surface area, which could relate to a direct increase in fixation strength and improved patient healing. The cross-over from periosteal to articular, and vice versa, could be reduced by 33.7% and 23.6% respectively. Because of this reduction in cross-over, machining time is saved by reducing redundant tool paths that would have repeated over 848 mm^2 of surface area. Furthermore, 10% of the periosteal surface was visible and accessible with the use of a tool containment boundary from the fracture setup angle, allowing for more complete machining of the periosteal surface.

Models 4, 5, and 6 represent smaller bone fragments each with only two different types of surfaces: periosteal and articular. No noise was present in the slices of these models, meaning noise removal had no impact on the setup angles, but tool containment boundaries still provide a significant benefit, which is shown in the following results for model 4. The setup angle solution for model 4 results in three angles: one angle for the periosteal surface and two different angles for the fractured

surface (Table 3.6.4, Model 4 Original). One of the fracture angles (112°) was very close to the periosteal angle (125°), overlapping with 99% of the periosteal surface. From the periosteal setup angle, 34% of the fracture surface was also visible (Figure 3.6.1). Machining from the periosteal angle would have removed 34% of the fracture surface, resulting in a significant loss in the initial fixation stability of the implant.

Table 3.6.4: Setup angles and cross-over statistics for model 4.

	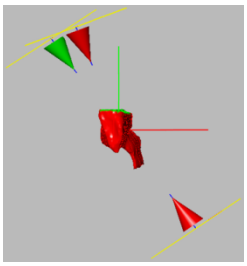	--	--
	Model 4 Original	Model 4 After Noise Removal	Model 4 With Tool Containment Boundaries
Noise Removed:	--	0.0 mm	--
Periosteal Angle:	125°	--	--
Fracture Angle:	112° and 306°	--	--
P to F:	34.2%	--	0% (-34.2%)
F to P:	99.1%	--	0% (-99.1%)
Redundant Machining	41.2%	--	0% (-41.2%)
Fracture Surface Improvement	--	--	34.2%

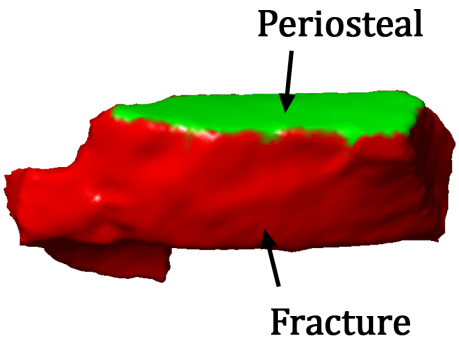

Figure 3.6.1: Model 4, viewed from the 125° periosteal angle, showing both periosteal and fracture surfaces visible.

With the use of tool containment boundaries, the periosteal and fracture surfaces in model 4 could be isolated from one another, allowing the fracture surface to be preserved and leading to a 34% increase in the initial fixation stability of the implant. Redundant machining can also be reduced by preventing the cutting tool from passing over the overlapping periosteal surface when machining from the fracture setup angle.

Model 5 is an interesting case. It is a simple model with mostly convex geometry, with a periosteal surface on one side and fracture surface on the opposite side (Figure 3.6.2). The setup angle solution resulted in only two angles: one each for the periosteal and fracture surfaces. The surfaces were completely isolated within their respective setup orientations, resulting in negligible surface overlap. In this model, the slice noise removal had no effect on the angles, and tool containment boundaries were also unnecessary.

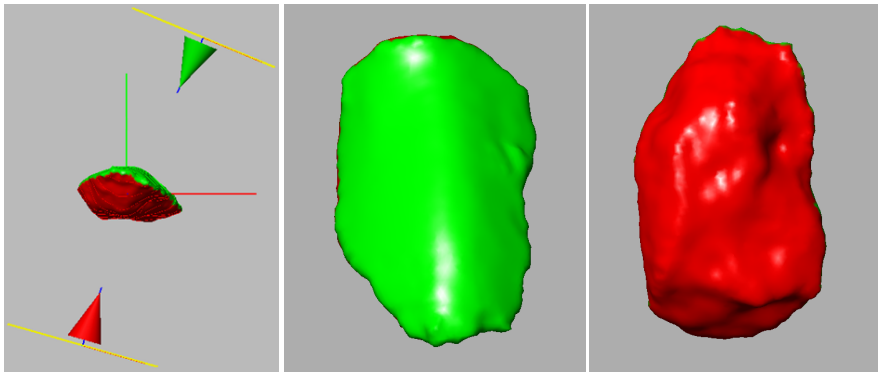

(a) (b) (c)

Figure 3.6.2: a) Side view of model 5 showing periosteal and fracture setup directions. b) View from the periosteal setup angle. c) View from the fracture setup angle.

In summary, the new methods had a significant impact, on average, for these samples. Although the degree of improvement varied, in the best case, 34% of the fracture surface could be preserved which may allow for increase fixation strength and improved healing time for the patient. In the next section, an example case is provided of actually machining an implant in surrogate bone material using the proposed methods for setup planning.

3.7 Machined Example

Model 1 was machined using the improved machining angles and tool containment boundaries generated from the program introduced in the previous section. The part was initially set up in Mastercam X4 using CNC-RP to perform hogging and rough machining operations. For the finishing operations on the part, improved setup angles were used that were calculated from the implementation presented in the previous section. The tool containment boundaries were also generated by the program developed for this thesis, traced in AutoCAD, and then imported into

Mastercam to be used as tool containment boundaries for the finishing operations of the part.

The resulting part shows a clear ability to control the surface finish on the different surfaces regions of the part, even if multiple surfaces are present in the same setup orientation (Figure 3.7.1). The red region shown in Figure 3.7.1b shows the 7.7% of the fracture surface that was visible from the 183° setup angle. Using tool containment boundaries, a rough surface finish was preserved on this area of the implant, increasing fixation stability for the patient.

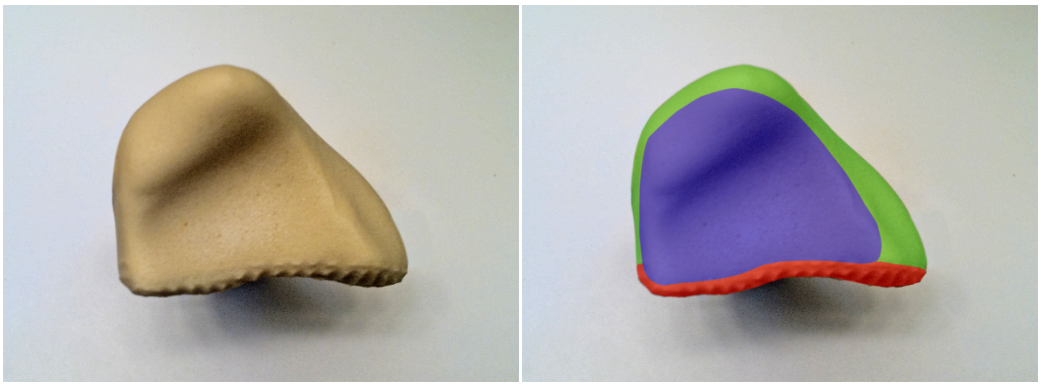

(a) (b)

Figure 3.7.1: Machined implant, viewed from the 183° setup orientation targeting the articular surface. Parts of the periosteal and fracture surfaces were visible and also machined from this orientation.

The same implant model was machined previously without the use of the tool containment boundaries, and is shown in Figure 3.7.2. While machining the articular surface, the visible portion of the fracture surface was also cut away (Figure 3.7.2a). This resulted in part of the fracture surface being smoothed away where it should have had a rough surface texture, as shown in the black out line in Figure 3.7.2b. This loss in

fracture surface customization can clearly be prevented in the new method using tool containment boundaries, as shown in Figure 3.7.1.

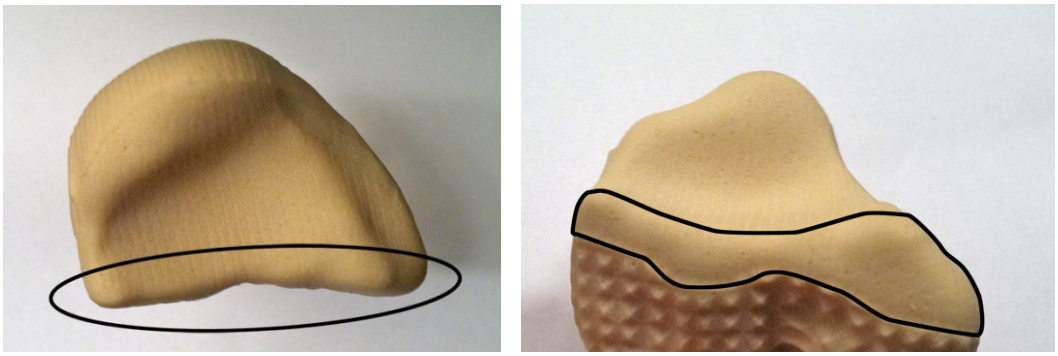

(a) (b)

Figure 3.7.2: Implant machined using previous methods, without tool containment boundaries. Missing fracture surface is outlined in black.

By isolating the surfaces with tool containment boundaries, part of the periosteal surface could also be machine from the same setup orientation as the fracture surface (Figure 3.7.3).

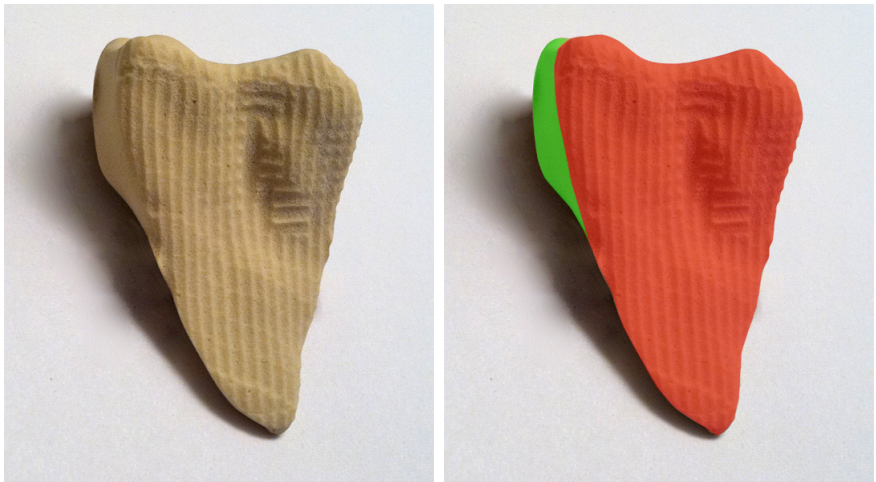

(a) (b)

Figure 3.7.3: Machined implant, viewed from the 62° setup orientation targeting the fracture surface. 10% of the periosteal surface was visible and also machined from this orientation.

The new methods for setup planning showed improved results over the previous method in preserving the fractured surface. Using tool containment boundaries, the cutting tool could be constrained to each type of surface without overlapping with another surface. This allowed for an increase in the customization of the fracture surface. In the next section, conclusions and future research directions are discussed.

3.7 Conclusion and Future Work

This research proposed new methods for providing customized surface characteristics in the rapid machining of patient-specific bone implants. Two problems were addressed: 1) How can one more accurately provide slice data for initial setup planning and 2) Given a set of setup angles, how can one ensure that the individual surfaces are machined independently? While addressing these problems, this work considered the overarching goal of ensuring that the biocompatibility of the implant is maintained. For the first problem, a method for modifying initial slice data was implemented that removed noise segments from the slices and allowed for improved machining angles to be found. Angles were found that helped reduce tool path crossover and allowed the cutting tool to be aimed more directly at the individual surfaces. To address the second problem, ensuring surfaces are independently machined, a method for constructing tool containment boundaries was implemented. The tool containment boundaries were able to constrain the cutting tool to each type of surface independently, ensuring that it does not inadvertently machine neighboring surfaces. The methods were used for performing setup planning for machining a bone

implant using a surrogate bone material. It was shown that the methods were effective at increasing the customization of the implant, showing a notable increase in the ability to customize the fracture surface.

An opportunity for future work would be to modify this approach so that is capable of handling many different types of surfaces, not limited to just three. Such an approach could be beneficial in custom industrial applications where more than three types of surfaces may appear in the same model. It may also be beneficial to store the facets of the model in a different type of data structure, instead of just storing the unstructured facet data reminiscent of STL files. For example, all facets corresponding to a certain type of surface could be stored independently from neighboring surfaces, with the facet data sorted and organized into "assemblies" of related color or geometry. A more structured format for the facet data may allow for more efficient computation.

References

[1] Albrektsson, T., C. Johansson. "Osteoinduction, osteoconduction and osseointegration." European Spine Journal (2001) 10:S96-S101.

[2] Melchels, Ferry P.W. and Feijen, Jan and Grijpma, Dirk W. (2010) "A review on stereolithography and its applications in biomedical engineering." Biomaterials, 31(24):6121-6130.

[3] Espalin, David, Karina Arcaute, David Rodriguez, et al. "Fused deposition modeling of patient-specific polymethylmethacrylate implants." Rapid Prototyping Journal (2010) 16:3:164-173

[4] Frank, M. C., C. V. Hunt, D. D. Anderson, T. O. McKinley, T. D. Brown. "Rapid Manufacturing in Biomedical Materials: Using Subtractive Rapid Prototyping for Bone Replacement." Proceedings of the Solid Freeform Fabrication Symposium (2008).

[5] Willert, H.G., G.H. Buchhorn. "Osseointegration of cemented and noncemented implants in artificial hip replacement: long-term findings in man." Journal of Long-Term Effects of Medical Implants (1999) 9(1-2):113-30.

[6] Le Guéhennec, L., A. Soueidan, P. Layrolle, Y. Amouriq. "Surface treatments of titanium dental implants for rapid osseointegration." Dental Materials (2007) 23:844-854

[7] Deglurkar, M., D. T. Davy, M. Stewart, V. M. Goldberg, J. F. Welter. "Evaluation of Machining Methods for Trabecular Metal Implants in a Rabbit Intramedullary Osseointegration Model." J Biomed Mater Res Part B: Appl Biomater (2006) 80B:528-540

[8] Grizon, F., E. Aguado, G. Huré, M.F. Baslé, D. Chappard. "Enhanced bone integration of implants with increased surface roughness: a long term study in sheep." Journal of Dentistry (2002) 30:195-203

[9] Rasmusson, L., Kahnberg, K.-E. and Tan, A. "Effects of Implant Design and Surface on Bone Regeneration and Implant Stability: An Experimental Study in the Dog Mandible." Clinical Implant Dentistry and Related Research (2001) 3:2–8.

[10] Cochran, D. L., R. K. Schenk, A. Lussi, et al. "Bone response to unloaded and loaded titanium implants with a sandblasted and acid-etched surface: A histomeric study in the canine mandible." Journal of Biomedical Materials Research (1998) 40:1-11.

[11] Sul, Y.T., C.B. Johansson, K. Röser, T. Albrektsson. "Qualitative and quantitative observations of bone tissue reactions to anodised implants" Biomaterials (2002) 23:1809-1817

[12] Kuiper, Jan Herman, Rik Huiskes, "Friction and Stem Stiffness Affect Dynamic Interface Motion in Total Hip Replacement" Journal of Orthopaedic Research (1996) 14:36-43

[13] Biemond, J.E., R. Aquarius, N. Verdonschot, P. Buma. "Frictional and bone ingrowth properties of engineered surface topographies produced by electron beam technology." Arch Orthop Trauma Surg (2011) 131:711-718

[14] Albrektsson, T., P.I. Branemark, H.A. Hansson, J. Lindström. (1981) "Osseointegrated Titanium Implants: Requirements for Ensuring Long-Lasting, Bone-to-Implant Anchorage in Man." Acta Orthopaedic 52:2:155-170

[15] Engh, C.A., J.D. Bobyn, A.H. Glassman. "Porous-coated hip replacement: the factors governing bone ingrowth, stress shielding, and clinical results." The Journal of Bone and Joint Surgery 69-B (1987):45-55

[16] Hsu, J.T., Chih-Han Chang, Heng-Li Huang, et al. "The number of screws, bone quality, and friction coefficient affect acetabular cup stability" Medical Engineering & Physics 29 (2007):1089-1095

[17] Sul, Young-Taeg. "The significance of the surface properties of oxidized titanium to the bone response: special emphasis on potential biochemical bonding of oxidized titanium implant." Biomaterials 24 (2003):3893-3907

[18] Puleo, D.A., A. Nanci. "Understanding and controlling the bone-implant interface." Biomaterials 20 (1999):2311-2321

[19] Joshi, Ashish. (2011). *Process planning for the rapid machining of custom bone implants*. M.S. Thesis. Iowa State University: U.S.A.

[20] Mendenhall, S. "Hip and knee implant review." Orthopedic Network News (2004) 15:1-16

[21] Thomas, Thaddeus P., Donald D. Anderson, et al. "A Computational/Experimental Platform for Investigating Three-Dimensional Puzzle Solving of Comminuted Articular Fractures." Computer Methods in Biomechanics and Biomedical Engineering (2010).

[22] Frank, M. C., R. A. Wysk, S. B. Joshi. "Determining Setup Orientations from the Visibility of Slice Geometry for Rapid Computer Numerically Controlled Machining." Journal of Manufacturing Science and Engineering (2006) 128:1:228-238

[23] Frank, M. C., R. A. Wysk, S. B. Joshi. "Rapid Planning for CNC Milling – A New Approach for Rapid Prototyping." Journal of Manufacturing Systems (2004) 23:3:242-255

[24] Frank, M.C. "Implementing Rapid Prototyping Using CNC Machining (CNC-RP) Through a CAD/CAM Interface." Proceedings of the Solid Freeform Fabrication Symposium (2007).

[25] Hieu, L.C., N. Zlatov, J. Vander Sloten, E. Bohez, L. Khanh, P.H. Binh, P. Oris, Y. Toshev, (2005) "Medical rapid prototyping applications and methods", Assembly Automation, Vol. 25 Iss: 4, pp.284 – 292.

[26] Chaikin, G. "An Algorithm for High Speed Curve Generation," Computer Graphics and Image Processing, vol. 4, no. 3, 1974.

[27] Dyn, Nira, David Levin, John A. Gregory, "A 4-point Interpolatory Subdivision Scheme for Curve Design," Computer Aided Geometric Design, vol. 4, no. 4, pp. 257-268, 1987.

[28] Piegl, Les, Wayne Tiller. The NURBS Book. 2nd Edition. New York: Springer. 1997. pp. 361-363.

[29] VCGLib, The VCG Library, http://vcg.sourceforge.net

[30] CGAL, Computational Geometry Algorithms Library, http://www.cgal.org

[31] Hinge Joint Image. Retrieved February 7, 2011 from http://www.stemcelltherapy.me/unit-three-model-of-a-working-limb/

Chapter 4: Conclusions and Future Work

This research proposed new methods for providing customized surface characteristics in the rapid machining of patient-specific bone implants. Two problems were addressed: 1) How can one more accurately provide slice data for initial setup planning and 2) Given a set of setup angles, how can one ensure that the individual surfaces are machined independently? While addressing these problems, this work considered the overarching goal of ensuring that the biocompatibility of the implant is maintained. For the first problem, a method for modifying initial slice data was implemented that removed noise segments from the slices and allowed for improved machining angles to be found. Angles were found that helped reduce tool path crossover and allowed the cutting tool to be aimed more directly at the individual surfaces. To address the second problem, ensuring surfaces are independently machined, a method for constructing tool containment boundaries was implemented. The tool containment boundaries were able to constrain the cutting tool to each type of surface independently, ensuring that it does not inadvertently machine neighboring surfaces. The methods were used for performing setup planning for machining a bone implant using a surrogate bone material. It was shown that the methods were effective at increasing the customization of the implant, showing a notable increase in the ability to customize the fracture surface.

In future research, it could be beneficial to modify the algorithms for finding setup angles to account for the fact that tool containment boundaries can now be used.

Instead of requiring angles that isolate the different surfaces, it may be beneficial in some cases to allow angles to overlap if it is desirable for a surface to be contacted at a steeper or shallower angle for applying a certain surface finish. Knowing that tool containment boundaries can be used, the angles could overlap an increasing amount (if desired) and the surfaces could still be isolated during machining.

Acknowledgements

I would like to thank Dr. Matthew C. Frank for all of his encouragement, patience, and help in the development of this thesis, and for his guidance in both my academic and professional careers. He both encouraged and challenged me on a daily basis, and this thesis would not have been possible without him. Thank you.

I would also like to thank Dr. Frank Peters for guiding me with optimism and positivity, and for giving me some of the best career advice I have ever received.

To Dr. Eliot Winer, thank you for serving on my committee and offering important insight from your experience with computer graphics, medical imaging, and CAD systems.

I would also like to thank Ashish Joshi and Rob DeGeorge for their constant help in the Rapid Manufacturing and Prototyping Laboratory (RMPL). Thank you Ashish, for your help and encouragement in writing this thesis.

This thesis also would not have been possible without the contributions of the following collaborators from the University of Iowa: Donald D. Anderson, PhD, Thaddeus P. Thomas, PhD, Yuki Tochigi, MD, PhD, M. James Rudert, PhD, J. Lawrence Marsh, MD, and Thomas D. Brown, PhD. This research was partly supported by grant funding from the National Institute of Arthritis and Musculoskeletal and Skin Diseases, National Institutes of Health, U.S. Department of Health & Human Services (AR055533, and AR054015).

References

[1] Albrektsson, T., C. Johansson. "Osteoinduction, osteoconduction and osseointegration." European Spine Journal (2001) 10:S96-S101.

[2] Melchels, Ferry P.W. and Feijen, Jan and Grijpma, Dirk W. (2010) "A review on stereolithography and its applications in biomedical engineering." Biomaterials, 31(24):6121-6130.

[3] Espalin, David, Karina Arcaute, David Rodriguez, et al. "Fused deposition modeling of patient-specific polymethylmethacrylate implants." Rapid Prototyping Journal (2010) 16:3:164-173

[4] Frank, M. C., C. V. Hunt, D. D. Anderson, T. O. McKinley, T. D. Brown. "Rapid Manufacturing in Biomedical Materials: Using Subtractive Rapid Prototyping for Bone Replacement." Proceedings of the Solid Freeform Fabrication Symposium (2008).

[5] Willert, H.G., G.H. Buchhorn. "Osseointegration of cemented and noncemented implants in artificial hip replacement: long-term findings in man." Journal of Long-Term Effects of Medical Implants (1999) 9(1-2):113-30.

[6] Le Guéhennec, L., A. Soueidan, P. Layrolle, Y. Amouriq. "Surface treatments of titanium dental implants for rapid osseointegration." Dental Materials (2007) 23:844-854

[7] Deglurkar, M., D. T. Davy, M. Stewart, V. M. Goldberg, J. F. Welter. "Evaluation of Machining Methods for Trabecular Metal Implants in a Rabbit Intramedullary Osseointegration Model." J Biomed Mater Res Part B: Appl Biomater (2006) 80B:528-540

[8] Grizon, F., E. Aguado, G. Huré, M.F. Baslé, D. Chappard. "Enhanced bone integration of implants with increased surface roughness: a long term study in sheep." Journal of Dentistry (2002) 30:195-203

[9] Rasmusson, L., Kahnberg, K.-E. and Tan, A. "Effects of Implant Design and Surface on Bone Regeneration and Implant Stability: An Experimental Study in the Dog Mandible." Clinical Implant Dentistry and Related Research (2001) 3:2–8.

[10] Cochran, D. L., R. K. Schenk, A. Lussi, et al. "Bone response to unloaded and loaded titanium implants with a sandblasted and acid-etched surface: A histomeric study in the canine mandible." Journal of Biomedical Materials Research (1998) 40:1-11.

[11] Sul, Y.T., C.B. Johansson, K. Röser, T. Albrektsson. "Qualitative and quantitative observations of bone tissue reactions to anodised implants" Biomaterials (2002) 23:1809-1817

[12] Kuiper, Jan Herman, Rik Huiskes, "Friction and Stem Stiffness Affect Dynamic Interface Motion in Total Hip Replacement" Journal of Orthopaedic Research (1996) 14:36-43

[13] Biemond, J.E., R. Aquarius, N. Verdonschot, P. Buma. "Frictional and bone ingrowth properties of engineered surface topographies produced by electron beam technology." Arch Orthop Trauma Surg (2011) 131:711-718

[14] Albrektsson, T., P.I. Branemark, H.A. Hansson, J. Lindström. (1981) "Osseointegrated Titanium Implants: Requirements for Ensuring Long-Lasting, Bone-to-Implant Anchorage in Man." Acta Orthopaedic 52:2:155-170

[15] Engh, C.A., J.D. Bobyn, A.H. Glassman. "Porous-coated hip replacement: the factors governing bone ingrowth, stress shielding, and clinical results." The Journal of Bone and Joint Surgery 69-B (1987):45-55

[16] Hsu, J.T., Chih-Han Chang, Heng-Li Huang, et al. "The number of screws, bone quality, and friction coefficient affect acetabular cup stability" Medical Engineering & Physics 29 (2007):1089-1095

[17] Sul, Young-Taeg. "The significance of the surface properties of oxidized titanium to the bone response: special emphasis on potential biochemical bonding of oxidized titanium implant." Biomaterials 24 (2003):3893-3907

[18] Puleo, D.A., A. Nanci. "Understanding and controlling the bone-implant interface." Biomaterials 20 (1999):2311-2321

[19] Joshi, Ashish. (2011). *Process planning for the rapid machining of custom bone implants*. M.S. Thesis. Iowa State University: U.S.A.

[20] Mendenhall, S. "Hip and knee implant review." Orthopedic Network News (2004) 15:1-16

[21] Thomas, Thaddeus P., Donald D. Anderson, et al. "A Computational/Experimental Platform for Investigating Three-Dimensional Puzzle Solving of Comminuted Articular Fractures." Computer Methods in Biomechanics and Biomedical Engineering (2010).

[22] Heiner, A.D., T.D. Brown (2007) "Frictional coefficients of a new bone ingrowth structure." Transactions of the 53rd annual meeting of the Orthopaedic Research Society, San Diego, California, USA, pp 1623.

[23] Frank, M. C., R. A. Wysk, S. B. Joshi. "Determining Setup Orientations from the Visibility of Slice Geometry for Rapid Computer Numerically Controlled Machining." Journal of Manufacturing Science and Engineering (2006) 128:1:228-238

[24] Frank, M. C., R. A. Wysk, S. B. Joshi. "Rapid Planning for CNC Milling – A New Approach for Rapid Prototyping." Journal of Manufacturing Systems (2004) 23:3:242-255

[25] Frank, M.C. "Implementing Rapid Prototyping Using CNC Machining (CNC-RP) Through a CAD/CAM Interface." Proceedings of the Solid Freeform Fabrication Symposium (2007).

[26] Li, Ye, M. C. Frank. “Computing non-visibility of convex polygonal facets on the surface of a polyhedral CAD model.” Computer-Aided Design (2007) 39:732-744

[27] Li, Ye, M. C. Frank. “Machinability Analysis for 3-axis Flat End Milling.” Journal of Manufacturing Science and Engineering (2006) 128:2:454-464

[28] Hieu, L.C., E. Bohez, J.V. Sloten, et al. “Design for medical rapid prototyping of cranioplasty implants.” Rapid Prototyping Journal (2003) 9:3:175-186.

[29] Hieu, L.C., E. Bohez, et al. “Design and manufacturing of cranioplasty implants by 3-axis CNC milling.” Technology and Health Care (2002) 10:5:413-423.

[30] Hieu, L.C., E. Bohez, et al. “Design and manufacturing of personalized implants and standardized templates for cranioplasty applications.” Proceedings from the IEEE International Conference on Industrial Automations (2002) 2:1025-1030

[31] Hieu, L.C., N. Zlatov, J. Vander Sloten, E. Bohez, L. Khanh, P.H. Binh, P. Oris, Y. Toshev, (2005) "Medical rapid prototyping applications and methods", Assembly Automation, Vol. 25 Iss: 4, pp.284 – 292.

[32] Choi, S.H., H.H Cheung. “Digital fabrication of multi-material biomedical objects.” Biofabrication 1 (2009).

[33] Choi, S.H., H.H Cheung. “Multi-material virtual prototyping for product development and biomedical engineering.” Computers in Industry 58 (2007):438-452.

[34] Choi, S.H., H.H Cheung. “A multi-material virtual prototyping system.” Computer-Aided Design 37 (2005):123-146.

[35] Wang, Chung-Shing, W.-H.A. Wang, M.-C. Lin. “STL Rapid prototyping bio-CAD model for CT medical image segmentation.” Computers in Industry 61 (2010):187-197.

[36] Wang, Dong-Xing, D.-M. Guo, Z.-Y. Jia, H.-W. Leng. “Slicing of CAD models in color STL format.” Computers in Industry 57 (2006):3-10.

[37] Zhou, M.Y., J.T. Xi, J.Q. Yan. “Modeling and processing of functionally graded materials for rapid prototyping.” Journal of Materials Processing Technology 146 (2004): 396-402.

[38] Kim, Dong Hwan, I.D. Yun, S.U. Lee. “Boundary-trimmed 3D triangular mesh segmentation based on iterative merging strategy.” Pattern Recognition 39 (2006):827-838.

[39] Latecki, L.J., R. Lakämper. “Convexity Rule for Shape Decomposition Based on Discrete Contour Evolution.” Computer Vision and Image Understanding (1999) 73:3:441-454.

[40] Hinge Joint Image. Retrieved February 7, 2011 from http://www.stemcelltherapy.me/unit-three-model-of-a-working-limb/